



Review

# Degradation of Residual Herbicide Atrazine in Agri-Food and Washing Water

Junting Hong<sup>1,2</sup>, Nadia Boussetta<sup>1</sup>, Gérald Enderlin<sup>1</sup>, Franck Merlier<sup>2</sup>  and Nabil Grimi<sup>1,\*</sup> 

<sup>1</sup> Université de Technologie de Compiègne, ESCOM, TIMR (Integrated Transformations of Renewable Matter), Centre de Recherche Royallieu, CEDEX CS 60319, 60203 Compiègne, France

<sup>2</sup> Université de Technologie de Compiègne, UPJV, CNRS, Enzyme and Cell Engineering, Centre de Recherche Royallieu, CEDEX CS 60319, 60203 Compiègne, France

\* Correspondence: nabil.grimi@utc.fr

**Abstract:** Atrazine, an herbicide used to control grassy and broadleaf weed, has become an essential part of agricultural crop protection tools. It is widely sprayed on corn, sorghum and sugar cane, with the attendant problems of its residues in agri-food and washing water. If ingested into humans, this residual atrazine can cause reproductive harm, developmental toxicity and carcinogenicity. It is therefore important to find clean and economical degradation processes for atrazine. In recent years, many physical, chemical and biological methods have been proposed to remove atrazine from the aquatic environment. This review introduces the research works of atrazine degradation in aqueous solutions by method classification. These methods are then compared by their advantages, disadvantages, and different degradation pathways of atrazine. Moreover, the existing toxicological experimental data for atrazine and its metabolites are summarized. Finally, the review concludes with directions for future research and major challenges to be addressed.

**Keywords:** atrazine; degradation; residue; agri-food; water



**Citation:** Hong, J.; Boussetta, N.; Enderlin, G.; Merlier, F.; Grimi, N. Degradation of Residual Herbicide Atrazine in Agri-Food and Washing Water. *Foods* **2022**, *11*, 2416. <https://doi.org/10.3390/foods11162416>

Academic Editor: Theodoros Varzakas

Received: 18 July 2022

Accepted: 9 August 2022

Published: 11 August 2022

**Publisher's Note:** MDPI stays neutral with regard to jurisdictional claims in published maps and institutional affiliations.



**Copyright:** © 2022 by the authors. Licensee MDPI, Basel, Switzerland. This article is an open access article distributed under the terms and conditions of the Creative Commons Attribution (CC BY) license (<https://creativecommons.org/licenses/by/4.0/>).

## 1. Introduction

Atrazine (Figure 1) is a triazine herbicide with a wide range of applications, for grassy and broadleaf weed control in corn, sugarcane, sorghum and certain other crops [1–4]. Due to its efficiency and low cost, its average consumption worldwide is 70,000 to 90,000 tons per year [5]. If shopping for conventional groceries, consumers are likely to have eaten food that has been sprayed with atrazine. Since atrazine is applied to crops used as livestock feed, its residues are found not only in crops, but also in milk and meat. According to the consumer risk assessment performed by the European Food Safety Authority [6], atrazine input values used for the dietary chronic exposure calculation of maize and other cereals except maize are 0.025 mg/kg and 0.05 mg/kg, respectively, based on the mean consumption data representative for 22 national diets. Although not considered acutely toxic to people, atrazine affects long term human health. Atrazine can act as the endocrine disrupting chemicals (EDC) [7] that can produce damage to the endocrine system, and cause a series of pathological changes and reproductive abnormalities [8]. Additionally, atrazine is also a potential carcinogen due to negative impact on human health such as tumors, breast, ovarian, and uterine cancers as well as leukemia and lymphoma [9]. For these reasons, atrazine was banned in the European Union (EU) in 2003 [10]. However, the commercial formulations of the herbicide atrazine (such as Gesaprim 90% WG) are still widely employed in Latin America. For example, herbicides were the main pesticide class used in Brazil between 2009 and 2018, with oscillations from 52.4% (2011) to 62.5% (2012), and atrazine was the top two active ingredient in this period [11]. Brazil is the world's third biggest exporter of agricultural products and organic food market leader in Latin America [12]. In addition, Brazil's main export markets are the European Union and the United States [13]. So, the residual problem of atrazine still remains a concern. Atrazine

is chemically stable with long half-life in water (30–100 days) [14,15], and its microbial degradation in soil environments is a relatively slow process (the range of field half-lives is 18 to 148 days [16,17]). It is also slightly soluble in water ( $33 \text{ mg}\cdot\text{L}^{-1}$  at  $22 \text{ }^\circ\text{C}$ ) and has low adsorption in soil [18]. Thus, it contaminates both surface and ground water [19]. The upper limit for atrazine in drinking water is  $3 \text{ }\mu\text{g}/\text{L}$  in America whereas in Europe, it is fixed as  $1 \text{ }\mu\text{g}/\text{L}$  [20,21]. However, investigations [22–24] have shown that concentrations of atrazine exceed the authorized limit of water contamination in surface water and ground water. Lots of works [25–28] have been conducted on the detection and quantification of atrazine in water, which is important to the food safety and quality control. Controlling the pollution of residual atrazine in agri-food and washing water has become a major issue.

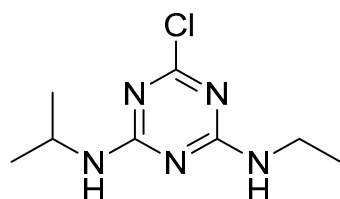


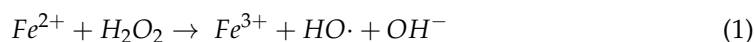
**Figure 1.** Atrazine (2-chloro-4-ethylamino-6-isopropylamino-1,3,5-triazine).

So far, many treatment technologies of aqueous atrazine have been developed, including microwave assisted photo reactions, advanced oxidation processes (AOPs), bioremediation, etc. This review summarizes recent degradation progress of atrazine in water, with an emphasis on current chemical methods (Fenton/Fenton-like Method [29–33], Sulfate Radical Oxidation [34–38], Photocatalytic Method [39–43], Electrocatalytic Method [44–48], Ozone Oxidation Method [49–53]), Biodegradation (Microbial Degradation [54–58] and Phytodegradation [59–63]) and physicochemical methods (High Voltage Electrical Discharges [64–69], Ultrasound [70–72], Microwave [73–75] and Ionizing Radiation [76–78]). Although two recently published reviews [79,80] also describe atrazine degradation techniques, they do not cover degradation methods comprehensively. This review not only expands the atrazine degradation techniques, but also compares them in terms of degradation pathways, atrazine mineralization, and metabolite toxicity.

## 2. Chemical Method

### 2.1. Fenton/Fenton-like Method

The classical Fenton reaction describes the activation of hydrogen peroxide ( $\text{H}_2\text{O}_2$ ) by ferrous ( $\text{Fe}^{2+}$ ) ions to generate hydroxyl radicals ( $\text{HO}\cdot$ ) [3]. The hydroxyl radical abstracts a hydrogen atom from organic substrate ( $\text{R}-\text{H}$ ), and generates an organic radical ( $\text{R}\cdot$ ), which subsequently undergoes a series of chemical transformation to form various oxidation products. The reactions are as follows:



Although the classic Fenton oxidation achieves the generation of free radicals and has strong oxidizing ability under ambient conditions, insoluble ferric hydroxide precipitates are generated during the process, which reduces the overall oxidation efficiency and requires continuous addition of  $\text{Fe}^{2+}$  salt. Therefore, Fenton-like methods with higher oxidation efficiency have been developed. For example, photo-Fenton, electro-Fenton and sono-Fenton are improvements of Fenton oxidation combined with photochemistry, electrochemistry, and ultrasound, respectively, and they have been used for the degradation of aqueous atrazine. In 2002, Ventura et al. [29] designed an electro-Fenton system and used it for the degradation of atrazine. The electro-Fenton system could continuously produce the ferrous iron and the hydrogen peroxide, thereby allowing more efficient generation of  $\cdot\text{OH}$ , which led to a more thorough oxidation of atrazine. In the same year,

Saltmiras et al. [30] published a similar work using anodic Fenton treatment to degrade 70% of atrazine in 3 min.

In 2020, Yang et al. [81] prepared a heterogeneous Fenton catalyst  $Fe/TiO_2$  using  $TiO_2$  synthesized by sol-gel method as carrier and ferric nitrate as  $Fe$  source, which could effectively remove atrazine under visible light, achieving over 95% removal efficiency within 30 min. In 2020, Shi et al. [82] reported  $Fe_3S_4$  Fenton oxidation of atrazine using visible light, and atrazine was completely degraded within 35 min. In 2021, Fareed et al. [83] adopted the  $UV/FeCl_3/H_2O_2$  system and achieved a 97% degradation rate of atrazine. In addition, the use of iron-modified mesoporous molecular sieve materials to degrade atrazine using UV-vis irradiation was reported by Benzaquén et al. [84]. Additionally, there are other related photo-Fenton systems, using tantalum (oxy)nitrides to prepare photocatalytic materials, on the degradation of aqueous atrazine [32,33,85,86].

The stepwise-Fenton's processes for the degradation of atrazine were developed by Chu et al. in 2007 [31]. And according to the system models built through the examination of reaction kinetics, they found that the performance of stepwise-Fenton's processes was better than that of conventional Fenton's processes.

## 2.2. Sulfate Radical ( $SO_4^-$ ) Oxidation Method

Compared with  $OH$ , the sulfate radical  $SO_4^-$  has a higher redox potential, longer half-life, and higher selectivity for electron transport reactions, receiving increasing attention on the degradation of pollutants [34]. So far, there are many generation methods of  $SO_4^-$  for atrazine removal (Table 1).

**Table 1.** Generation methods of  $SO_4^-$  for atrazine removal.

Generation Methods	Removal Effect
Carbon sheet fabricated from corn straw and potassium oxalate activated persulfate.	97.2% of atrazine was removed by the system within 20 min, when the concentration of persulfate was 2 mM [34].
Biochar supported nZVI composites (nZVI@BC) activated persulfate.	The atrazine removal rate was up to 93.8% [35].
Siderite/ $CaSO_3$ system was used to provide $Fe^{2+}$ to activate sulfite.	>90% atrazine was removed within 6 min at 45 °C [36].
Pyrite activated persulfate.	100% of atrazine was degraded in 45 min and the TOC (total organic carbon) removal efficiency was 26% within 7 h [37].
Mechano chemically synthesized S-ZVI <sup>bm</sup> composites activated persulfate.	The degradation of atrazine was up to 90%, which was pH-independent [38].
Nanoscale $LaFe_{1-x}Cu_xO_{3-\delta}$ perovskite activated peroxymonosulfate.	Atrazine (23 $\mu$ M) was removed completely within 60 min in the presence of 0.5 g/L catalyst and 0.5 mM peroxymonosulfate [87].
Composite of nanoscale zero valent iron and graphene activated persulfate.	92.1% of atrazine was removed within 21 min using mass ratio of 5:1 nanoscale zero-valent iron (nZVI) to graphene (GR) [88].
Natural negatively-charged kaolinite with abundant hydroxyl groups activated peroxymonosulfate.	When the kaolinite dosage increased to 1.0 g/L, the degradation of atrazine exceeded 90% at 60 min [89].
Cobalt-impregnated biochar activated peroxymonosulfate.	99% of atrazine was degraded within 6 min [90].
Co-doped mesoporous $FePO_4$ activated peroxymonosulfate.	100% of atrazine was degraded for CoFeP-0.1 after 30 min at pH = 7 [91].
$LaCoO_3/Al_2O_3$ activated peroxymonosulfate.	Under the optimal conditions, the removal rate and mineralization efficiency of ATZ reached 100% and 30.8%, respectively [92].
Copper sulfide activated persulfate.	The degradation of atrazine was up to 91.6% [93]

Table 1. Cont.

Generation Methods	Removal Effect
Hydroxylamine drinking water treatment residuals activated peroxymonosulfate.	The removal efficiency of atrazine was 95.5% in 30 min [94].
Fe <sub>3</sub> O <sub>4</sub> -sepiolite activated persulfate.	71.6% of atrazine and 20% of solution TOC were removed after 60 min [95].
CoMgAl layered double oxides activated peroxymonosulfate.	The degradation of atrazine was up to 98.7% [96].

In addition, there are processes that combine sulfate radical oxidation with other technologies such as UV-vis [97,98]. The photocatalysis technology is needed for the activation of sulfite to generate  $SO_4^-$  effectively at the neutral pH condition without any precipitation of metal-hydroxyl species, thus greatly improving the degradation rate of atrazine.

### 2.3. Photocatalytic Method

Photocatalysis generally refers to a photochemical reaction with the participation of a catalyst. Under the irradiation of ultraviolet or visible light, electron–hole pairs are created by photocatalysts, which generate free radicals such as  $OH$  able to oxidize and decompose organic pollutants. The image below (Figure 2) refers to reference [99].

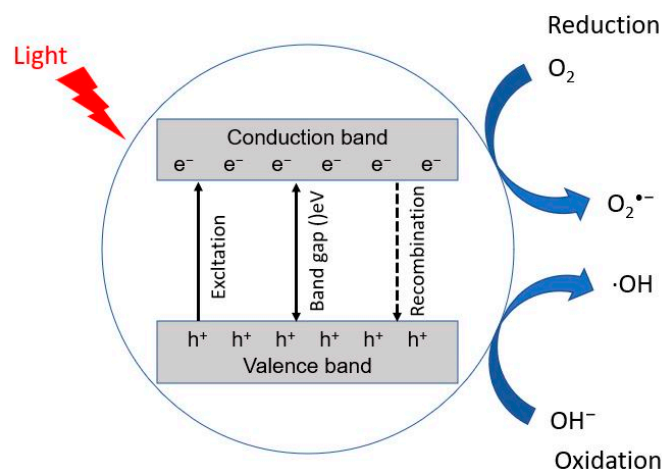


Figure 2. Schematic representation of mechanism of photocatalysis.

The general photocatalysts are N-type semiconductor materials, which have the characteristics of low band gap, such as  $TiO_2$ ,  $ZrO_2$ ,  $ZnO$ ,  $CdS$ ,  $WO_3$ ,  $Fe_2O_3$ ,  $Bi_2O_3$ , etc. Among them, *Ti*-based, *W*-based, and *Bi*-based materials and their oxides are commonly used in the photodegradation of aqueous atrazine (Table 2).

In addition, photoelectrocatalysis (PEC), which combines both electrochemistry and photocatalysis, has also been used in the degradation of aqueous atrazine. In 2018, Fernández-Domene et al. [100] reported the degradation of atrazine by photo-electrocatalysis using a photoanode based on  $WO_3$  nanosheets. Atrazine was completely degraded after 180 min. In 2021, Xie et al. [101] used the bias potential applied on the photo-anode to achieve a 96.8% removal efficiency of atrazine.

The photocatalytic method has received widespread attention because of its high efficiency, non-toxicity, and lack of secondary pollution. It is recommended to use visible light catalytic process to degrade atrazine, because the use of solar energy is sustainable and environmentally friendly.

**Table 2.** Photodegradation of aqueous atrazine.

Photocatalyst	Preparation	Light Source	Removal Effect
In, S-TiO <sub>2</sub> @rGO nanocomposite	TiO <sub>2</sub> @rGO nanocomposites were synthesized based on a new ultrasonic-assisted hydrothermal method.	Visible-light, a 300 W tungsten xenon lamp.	The complete degradation and 95.5% mineralization of atrazine was achieved within 20 min [39].
Boron-doped TiO <sub>2</sub>	Used a one-step calcination method.	Visible-light, a 350 W (15 A) Xenon lamp with a 300 nm cutoff filter (CHF-XM-350 W, Beijing Trusstech. Co., Beijing, China).	The degradation of atrazine was up to 95% [40].
Metalloporphyrins supported on TiO <sub>2</sub>	Tetra (4-carboxyphenyl) porphyrin with different metal centers and metal-free was adsorbed on TiO <sub>2</sub> surface.	Visible-light, an open borosilicate (Pyrex) glass cell with an optical window of 11 cm <sup>2</sup> area.	82% of atrazine was degraded using Cu(II) porphyrin within 1 h [41].
Crystal TiO <sub>2</sub> nanowires with high specific surface area	Use a PEG-assisted hydrothermal method.	UV irradiation, two 15 W Philips UV light lamps (365 nm wavelength, intensity: 2.47 ± 0.16 mW cm <sup>-2</sup> ).	The degradation of atrazine is up to 60% in 1 h [42].
TiO <sub>2</sub> nanoparticles involved boron enrichment waste		UV irradiation, a UV lamp (400 W, λ = 250–570 nm).	The degradation of atrazine is up to 60% in 70 min. The removal of atrazine followed a pseudo-first-order reaction kinetic [43].
Mesoporous Ag-WO <sub>3</sub> /SBA-15 composite		Visible-light, a broadband light source (450 W Xe arc lamp) fitted with a neutral density optical filter to allow light of wavelength above 400 nm.	70% of atrazine was degraded in 18 min [102].
Heterojunction BiVO <sub>4</sub> -Bi <sub>2</sub> O <sub>3</sub>	Platelet-like BiVO <sub>4</sub> was synthesized by hyperbranched polyethyleneimine [103].	Visible-light, a mercury 250 W High-Pressure lamp.	The heterojunction efficiently removed >90% of atrazine [104].
CdS/BiOBr/Bi <sub>2</sub> O <sub>2</sub> CO <sub>3</sub> ternary heterostructure materials	Used a simple one pot hydrothermal method.	Visible-light, a 250 W xenon lamp with a 400 nm cutoff filter.	The degradation of atrazine was up to 95% in 30 min [105].
BiOBr/UiO-66 composite	Used an in situ growth method.	Visible-light, a 300 W Xe lamp (Beijing Zhongjiaojinyuan, CEL-HXF300) with a 400 nm cut-off glass filter.	The degradation of atrazine was up to 90% in 3 h [106].
Cu-BiOCl	Used a one-pot solvothermal method.	UV irradiation, a Steripen Mercury UV lamp with emission wavelength of 254 nm.	29% of atrazine was degraded [107].

#### 2.4. Electrocatalytic Method

Electrocatalysis is a catalytic process involving oxidation and reduction reactions through the direct transfer of electrons, which requires electrocatalysts to lower the overpotential of the reactions [108]. Electrocatalytic oxidation technology can produce ·OH in situ and no additional chemical reagent is required, which can remove atrazine from wastewater efficiently and environmental-friendly [44]. Electrode materials play an essential role in the

progress of electrocatalytic oxidation. Various types of electrodes have been exploited for the degradation of atrazine in water (Table 3).

**Table 3.** Electrocatalytic oxidation of aqueous atrazine.

Electrodes	Removal Effect
Co/Sm-modified Ti/PbO <sub>2</sub> anode	The maximum degradation rate of 92.6% and the chemical oxygen demand (COD) removal rate of 84.5% are achieved in electrolysis time 3 h [44].
Fly ash-red mud particle electrode	90.1 % atrazine was degraded in 30 min [45].
Bifunctional nickel foam composite cathode co-modified with CoFe@NC and CNTs	The removal of atrazine reached 100% in 105 min under the given conditions, the removal efficiency of TOC after 420 min was $78.7 \pm 2.6\%$ [46].
Boron Doped Diamond (BDD) anode	Around 100% removal rate of atrazine was achieved in 4 h [47].
BDD anode	Permanganate was in situ electrochemical generated for the treatment of atrazine. Atrazine degradation increased significantly with permanganate production [48].
BDD anode	A high mineralization rate of 82% was obtained [18].
BDD, Carbon Felt, and Mixed Metal Oxides Anodes with Iridium and Ruthenium	BDD completely removes atrazine, and rest of anodes reached approximately 75% atrazine removal [109].

In addition, electrochemistry has also been combined with ozone oxidation to degrade aqueous atrazine [110]. In 2016, Zhou et al. proposed a novel oxidation process using iron electrodes and ozone in atrazine degradation [111]. Moreover, atrazine degradation by in situ electrochemically generated ozone was reported by Vera et al. in 2009 [112]. The combination of electrochemistry and ozonation exhibited higher removal efficiency for ATZ than ozonation and electrocoagulation [111].

Moreover, Electrochemical Advanced Oxidation Processes (EAOPs) is also an efficient method to remove recalcitrant molecules. Atrazine is a very stable molecule with a relative resistance to microbial attack. Therefore, EAOPs can be used for pretreatment, before the biodegradation of atrazine [109].

### 2.5. Ozone Oxidation Method

Ozone is a strong oxidant, which can oxidize organic or inorganic substances in wastewater, thereby disinfecting, oxidizing or decolorizing. Because atrazine is resistant to the degradation by ozone, additional catalysts are required for the ozonation of atrazine [113]. In recent years, the ozonation of aqueous atrazine has been reported (Table 4).

In addition, using ozone oxidation combined with other oxidation processes can improve the degradation efficiency and mineralization rate of atrazine. In 2006, Bianchi et al. [114] studied the mechanism of atrazine degradation in aqueous phase under sonolysis at 20 kHz, ozonation, photolysis at 254 nm and photocatalysis in the presence of TiO<sub>2</sub>, employed either separately or in combination. Ozonation and photocatalysis induced atrazine de-alkylation, followed by slower de-chlorination, and simultaneous sonolysis increased the rate of photocatalytic de-alkylation. The highest degradation rate of atrazine was achieved when photolysis at 254 nm was combined with ozonation.

**Table 4.** Ozonation of aqueous atrazine.

Catalyst	Removal Effect
Manganese	The presence of humic substances has a substantial influence on the Mn-catalysed ozonation of atrazine [49].
A non-ionic surfactant, Brij35 (polyoxyethylene (23) lauryl ether)	Atrazine was completely removed after a reaction time of 2 h [50].
Nano-ZnO	The degradation efficiency of atrazine was 99% after 5 min reaction at pH 6 [51].
Mesoporous Fe <sub>3</sub> O <sub>4</sub>	The removal rate of atrazine was up to 97% [52].
Hydroxylamine	80% of atrazine was degraded by ozonation in the presence of hydroxylamine [53].
Rutile TiO <sub>2</sub>	The removal rate and the mineralization of atrazine was 93% and 56%, respectively [115].
Oxygen functionalized graphitic carbon nitride O@g-C <sub>3</sub> N <sub>4</sub>	The removal rate of atrazine was 93%, after 5 min reaction at pH 6 [116].
Three-dimensional Co/Ni bimetallic organic frameworks	94% of atrazine were removed [117].

### 3. Biodegradation

Biodegradation refers to the partial, and sometimes total, transformation or detoxification of contaminants by microbial, plants or enzymes [118]. It has advantages over physical and chemical methods in terms of low costs and environmental friendliness [119]. Since the discovery of biotic atrazine degradation [120,121], biodegradation has been a major method for atrazine catabolism [1].

#### 3.1. Microbial Degradation

Microbial degradation exploits the ability of microorganisms for removal of pollutants from contaminated sites [122]. That is because indigenous microorganisms that are already present in polluted environments may transform pollutants to harmless products via reactions that take place as a part of their metabolic processes [123]. Generally, isolated microbes are selected for the degradation due to nature and type of pollutants. Different atrazine-degrading bacteria and fungi have been isolated (Table 5). Because microorganisms are easily drained in water making their effectiveness greatly reduced, Yu et al. [58] developed a self-immobilized biomixture (SIB) with biosorption and biodegradation properties, that can obtain better atrazine removal rate.

**Table 5.** Microbial degradation of aqueous atrazine.

Strain	Origin	Removal Effect
<i>Arthrobacter</i> sp. DNS10	Black soil [54]	The removal rate of 100 mg/L atrazine reached 95% and 86% in 0.05 mM Zn <sup>2+</sup> and 1.0 mM Zn <sup>2+</sup> , respectively at 48 h [55].
<i>Bacillus badius</i> ABP6	Maize fields	Response-surface-methodology (RSM) was used to optimize environmental factors such as pH, temperature, agitation speed and atrazine-concentration on atrazine degradation by utilizing <i>Bacillus badius</i> ABP6 strain. In the optimum conditions (pH 7.05, temperature 30.4 °C, agitation speed 145.7 rpm, and atrazine-concentration 200.9 ppm), the degradation rate of atrazine reaches a maximum value of 90% [56].

Table 5. Cont.

Strain	Origin	Removal Effect
<i>Bjerkanderaadusta</i>	Rotten wood surfaces	In the optimum conditions (pH 4, temperature 28 °C, biomass 2 g, and atrazine-concentration 50 ppm), the removal rate of atrazine was up to 92% in 5 days [57].
<i>Agrobacterium</i> sp. WL-1, <i>Arthrobacter</i> sp. ZXY-2	Jilin Pesticide Plant	After adding biochar ZXY-2 pellets, the removal rate of atrazine reached 61% within 1 h, higher than that treated by ZXY-2 pellets without biochar. The addition of biochar could enhance the connection between ZXY-2 and pellets-based carrier, and the favorable biodegradation pH of ZXY-2 changed to 6 and 10 [58].
<i>Chlorella</i> sp.	The Freshwater Algae Culture Collection at the Institute of Hydrobiology, China	Atrazine with initial concentration of 5 mg/L was photocatalytic degraded for 60 min with degradation ratio of 31%. After an 8 d exposure of the microalga <i>Chlorella</i> sp., 83% and 64% of the atrazine were removed from the degraded solutions containing 40 µg/L and 80 µg/L of atrazine, respectively [124].
<i>Myriophyllum spicatum</i>	Wuhan Botanical Garden	<i>Myriophyllum spicatum</i> absorbed more than 18-fold the amount of atrazine in sediments and degraded atrazine to hydroxyatrazine (HA), deethylatrazine (DEA), didealkylatrazine (DDA), cyanuric acid (CYA) and biuret. The formation of biuret suggested for the first time, the ring opening of atrazine in an aquatic plant. The residual rate of atrazine was $6.5 \pm 2.0\%$ in <i>M. spicatum</i> -grown sediment on day 60 [125].

### 3.2. Phytodegradation

The phytodegradation of organic compounds take place inside the plant or within the rhizosphere of the plant [126]. Rhizosphere, the immediate vicinity of plant roots, is a zone of intense microbial activity, and the use of vegetation at the waste sites can overcome the inherent limitations such as low microbial population or inadequate microbial activity [59]. It has been reported that atrazine can be degraded or detoxified in crops [60,61], and the molecular mechanism for catabolism and detoxification of atrazine in plants is a major research topic (Table 6).

Table 6. Phytodegradation of aqueous atrazine.

Plant	Gene/Enzymes	Result
<i>Pennisetum claudatum</i>	Soil dehydrogenase	Within 80 days, nearly 45% of atrazine was degraded [59].
Rice	Two novel methyltransferases LOC_Os04g09604, LOC_Os11g15040	Atrazine degradation and detoxification are regulated [62]
Alfalfa ( <i>Medicago sativa</i> )	Genes encoding glycosyltransferases, glutathione S-transferases or ABC transporters	Atrazine in alfalfa can be detoxified through different pathways [63].

Generally, atrazine may be degraded within the plant biomass by plant enzymes as well as in its rhizosphere by microbial biotransformation [127,128].



## 4. Physicochemical Method

### 4.1. High Voltage Electrical Discharges (HVED)

High Voltage Electrical Discharges (HVED) is one of the advanced oxidation processes that has been used for the treatment of wastewater. During the discharge processes of gas and liquid system, the low-temperature plasma, high-energy electrons and UV-radiation are generated to degrade wastewater. The generated plasma is a conductive fluid that is electrically neutral and consists of electrons, positive and negative ions, free radicals, neutral particles and excited-state atoms [129]. Among them, the high-energy electrons bombard water molecules to ionize and generate oxidants such as  $\cdot OH$  and  $H_2O_2$ , which can efficiently degrade organic substances. The main reactions include:



The plasma reactors can be divided into three types. One is the non-thermalizing electrical discharge applied in the air above an aqueous solution, generating an atmospheric plasma. The second is the discharge applied into the water, creating high-temperature plasma channels. In addition, the hybrid reactors utilize both gas phase nonthermal plasma formed above the water solution and direct liquid phase corona-like discharge in water [130].

In 1997, Houben et al. [64] reported a research work on the degradation of atrazine by pulsed corona discharges above the water surface, in which 0.12 mM atrazine was oxidized for 5 h and the degradation rate was 57%. This is the earliest work using plasma reactors to degrade atrazine. Several years later, in 2005, Karpel Vel Leitner et al. [65] applied the pulsed arc electrohydraulic discharge (PAED) system on the degradation of atrazine. PAED was generated by a spark gap type power supply (0.5 kJ/pulse) with rod-to-rod type electrodes in water. The removal rate of atrazine (0.5  $\mu\text{mol/L}$ ) achieved 80% with inter-electrode gap of 4 mm when the input energies were higher than 10 kJ/L. In 2007, Mededovic and Locke [66] present an investigation of the atrazine degradation by pulsed electrical discharge in water. Different electrolytes and electrode materials were studied. An initial pH 3 (adjusted with  $H_2SO_4$ ) 90% of the atrazine ( $2 \times 10^{-5}$  M) was degraded in 1 h, and the final degradation product was ammeline. When ferrous ions were used as an electrolyte, atrazine was degraded within 10 min due to the hydrogen peroxide produced by the discharge which reacted with ferrous ions. In addition, they compared their work with the above two pulsed electrical discharge works. The comparison of energy efficiency showed that the underwater pulsed electrical discharge had higher atrazine conversion for the same energy input than discharge above the water surface and pulsed arc discharge (Table 7).

**Table 7.** Comparison of energy efficiency for the three pulsed electrical discharge processes.

Technology	Concentration of Atrazine (M)	Energy Efficiency (mol/J)
Pulsed electrical discharge in water [66]	$2 \times 10^{-5}$	$3 \times 10^{-9}$
Pulsed corona discharges above the water surface [64]	$0.12 \times 10^{-3}$	$7.67 \times 10^{-10}$
Pulsed arc electrohydraulic discharge in water [65]	$2 \times 10^{-6}$	$1.56 \times 10^{-10}$

Moreover, there are four other works using dielectric barrier discharge (DBD), a typical non-equilibrium high-voltage gas discharge. In 2014, Zhu et al. [67] designed a novel wire-cylinder DBD plasma reactor for atrazine degradation, and the degradation rate was up to 93.7%, and 12.7% of total organic carbon (TOC) was removed after 18 min of discharge at the optimum conditions (input power = 50 W, air flow rate = 140 L·h<sup>-1</sup>). In 2015, Patrick Vanraes et al. combined DBD with absorption of activated carbon [69] or nanofiber membrane [68] on the degradation of atrazine. In 2021, Wang et al. [131] combined DBD with microbubbles (MBs) for persulfate (PS) activation and atrazine removal in water. Under these DBD/MBs/PS systems, the degradation efficiency reached 89% after 75 min of treatment at a discharge power of 85 W, a PS concentration of 1 mM, and an air flow rate of 30 mL/min. And according to the calculated energy yield (EY 41.8 mg/kWh at a discharge power of 85 W), they supposed that DBD/MBs/PS system was economically viable in treating large scale atrazine wastewater.

In addition, there is another report on the remediation of atrazine in a plasma reactor. In 2018, Aggelopouloset al. [132] used DBD plasma at atmospheric air pressure to treat a sandy soil polluted with atrazine. The atrazine degradation rates of 87% and 98% were achieved after 60 min of plasma treatment, starting from initial pollutant concentrations of 100 and 10 mg/kg, respectively.

HVED is an innovative technique, which combines sonochemistry, high-energy electron radiation, photochemistry, etc., and can effectively decompose organic pollutants. Nevertheless, the use of HVED for wastewater treatment is still under development, and further research is needed. The research on the degradation behavior of aqueous atrazine by plasma deserves more attention.

#### 4.2. Ultrasound

The main principles of ultrasonic degradation of pollutants in water are cavitation effect and free radical oxidation. The high energy generated by the collapse of the ultrasonic cavitation bubble is sufficient to break the chemical bond and generate hydroxyl radicals ·OH and hydrogen radicals ·H, which oxidize organic substances and transform into CO<sub>2</sub>, H<sub>2</sub>O, inorganic ions or low-toxic organic compounds. At the same time, the rupture of bubbles enhances the purification. In wastewater treatment, ultrasound technique is often combined with other techniques [133] (ozone oxidation, ultraviolet irradiation, biodegradation, etc.) to achieve efficient degradation.

The earliest report on ultrasonic treatment of aqueous atrazine was reported by W.C. Koskinen et al. in 1994 [134], and the kinetic of sonochemical decomposition of atrazine in water was determined. In 1996, Petrier et al. [70] used two frequencies (20 kHz and 500 kHz) to degrade atrazine in aqueous solution. The degradation rate of atrazine was nearly 100% after 80 min at 500 kHz and 55% after 120 min at 20 kHz.

Later, ultrasonic treatment was combined with other techniques to degrade aqueous atrazine, and it is common to combine US and UV, or US and ozonation. In 2001, A. Hiskia et al. [135] published a report on US/UV decomposition of atrazine in the presence of polyoxometalates (POM) within a few minutes, giving common intermediates, namely, 2-hydroxy-4-(isopropylamino)-6-(ethylamino)-s-triazine (HA), 2-chloro-4-(isopropylamino)-6-amino-s-triazine (DEA), 2-chloro-4-amino-6-(ethylamino)-s-triazine (DIA), ammeline (AM) among others. The final products for both methods, US and UV with POM, were cyanuric acid, NO<sub>3</sub><sup>-</sup>, Cl<sup>-</sup>, CO<sub>2</sub>, and H<sub>2</sub>O. In 2012, R. Kidak and S. Dogan [136] investigated the efficiency of O<sub>3</sub> and US and also of their combined application (US + O<sub>3</sub>) for the degradation and potential mineralization of atrazine in water, leading to 95% removal for O<sub>3</sub> and 78% for US after 90 min of treatment, and 100% for US + O<sub>3</sub> after 20 min of treatment. In 2014, Xu et al. [71] reported sonophotolysis (US/UV) for the degradation of atrazine. After 60 min of sonophotolysis treatment, the complete degradation of atrazine and 60% total organic carbon (TOC) removal rate were achieved. In 2017, Jing et al. [72] used a pilot-scale UV/O<sub>3</sub>/US flow-through system to remove atrazine from wastewater. The optimal

atrazine removal rate (98%) was obtained at the conditions of 75 W UV power, 10.75 g·h<sup>-1</sup> O<sub>3</sub> flow rate and 142.5 W ultrasound power.

Ultrasonic treatment has a strong effect on the degradation of organic substances, but it has the problem of high energy consumption. For the degradation of aqueous atrazine, more consideration can be given to combine ultrasonic treatment with other techniques, such as biodegradation, electrochemistry, Fenton oxidation, etc.

#### 4.3. Microwave

Microwave treatment is a breakthrough, innovative, and broad-spectrum water treatment technique. It achieves the effect of decontamination and sterilization through the selective heating, low-temperature catalysis, and rapid penetration by the microwave field. The principle is that microwave heating generates efficient internal heat-transfer by penetrating subjects and causing uniform energy distribution throughout the material irradiated, which leads to an even chemical reaction [137]. Microwave irradiation can cause atrazine degradation through formation of micro-scale “hot spots” on the pore wall surface that pyrolyze the absorbed organic molecules [138].

In existing reports, microwave is often used as an auxiliary technique for the treatment of atrazine. The earliest work was on the microwave-assisted extraction of atrazine from soil, reported by Xiong et al. [73] in 1998. The combination of microwave (MW) power and ultraviolet (UV) light can improve the photochemical process, thereby making the degradation of atrazine more efficient. In 2006, Ta et al. [74] reported the degradation of atrazine by microwave-assisted electrodeless discharge mercury lamp (MW-EDML) in aqueous solution. Microwave improved the photolysis of atrazine under UV-vis irradiation, so that it was completely degraded in a relatively short time (i.e.,  $t_{1/2} = 1.2$  min for 10 mg/L). Additionally, the main degradation products during atrazine degradation process were identified by gas chromatography mass spectrometry (GC-MS) and liquid chromatography mass spectrometry (LC-MS), according to which the degradation mechanism including four possible pathways for atrazine degradation was proposed. In 2007, Gao et al. [75] reported a method of microwave-assisted photocatalysis on TiO<sub>2</sub> nanotubes for the degradation of aqueous atrazine. Atrazine was completely degraded in 5 min and the mineralization efficiency was 98% in 20 min, which superior to many other atrazine degradation works (they cannot achieve complete atrazine degradation with the formation of many toxic intermediates such as Deethylatrazine, Deisopropylatrazine, ammeline, etc.). High mineralization efficiency means that atrazine was released in soluble inorganic forms such as CO<sub>2</sub>, H<sub>2</sub>O, NH<sub>4</sub><sup>+</sup> and small acids, which is beneficial to the non-toxic treatment of wastewater. Therefore, for the degradation of atrazine, not only a high degradation efficiency, but also a high mineralization rate is very important. In 2011, Chen et al. [139] used a microwave photochemical reactor to degrade atrazine in the presence of hydrogen peroxide H<sub>2</sub>O<sub>2</sub>. The optimal condition of atrazine degradation by MW/UV/H<sub>2</sub>O<sub>2</sub> process was 53 °C, 300 mg/L H<sub>2</sub>O<sub>2</sub>, MW power  $P_{\text{appl}} = 30 \pm 0.3$  W (half-life  $t_{1/2} = 1.1$  min for 20.8 mg/L initial concentration). Comparing with other processes such as UV alone [139] (half-life  $t_{1/2} = 9.9$  min for 20 mg/L initial concentration), UV/H<sub>2</sub>O<sub>2</sub> [140] (half-life  $t_{1/2} = 1.2$  min for 8.4 mg/L initial concentration with 343.4 mg/L H<sub>2</sub>O<sub>2</sub>) and MW/UV [139] (half-life  $t_{1/2} = 2.2$  min for 20.8 mg/L initial concentration), microwave-assisted photocatalytic method is better than traditional photocatalytic methods, and adding H<sub>2</sub>O<sub>2</sub> can achieve high-efficiency degradation of aqueous atrazine.

In addition, for traditional adsorption, its degradation efficiency highly depends on the adsorbent, while microwave heating can modify the adsorbent to bring about highly efficient adsorbent performance. Therefore, the adsorption and degradation of aqueous atrazine under microwave heating has attracted attention. Hu et al. [138,141] reported the adsorption and degradation of atrazine in transition metal-loaded microporous under microwave induction. In 2017, Wei et al. [142] enhanced adsorption of atrazine using a coal-based activated carbon modified with sodium dodecyl benzene sulfonate under microwave heating. In the same year, Sivarajasekar et al. reported a fixed-bed column

towards sorptive removal of Atrazine from aqueous solutions using microwave irradiated Aegle marmelos Correa fruit shell.

#### 4.4. Ionizing Radiation ( $\gamma$ -Rays, Electron Beams)

In recent years, due to environmental protection, ionizing radiation treatment of pollutants has received more and more attention. Ionizing radiation can cause displacement of electrons from atoms and breaks in chemical bonds, and  $\gamma$ -rays and electron beams are most commonly employed forms [143].

In 2009, Basfar et al. [76,77] reported the degradation of atrazine herbicide in humic substances (HS) aqueous solutions and distilled water solutions on a laboratory scale upon  $\gamma$ -irradiation from a  $^{60}\text{Co}$  source, which can achieve 90% degradation rate of atrazine. And they later use  $\gamma$ -irradiation to degrade atrazine present in natural ground waters on a laboratory scale.

In 2015, Khan et al. [78,144] studied the kinetics, degradation pathways, influence of hydrated electron and radical scavengers in the degradation of aqueous atrazine by  $\gamma$ -irradiation, and the degradation rate can reach 69% under optimal conditions.

In addition, electron beams induced degradation of atrazine in aqueous solution was reported by Xu et al. [145] in 2015. Atrazine can be almost completely degraded (95%) and completely mineralized without any residue of cyanuric acid in aqueous solution.

### 5. Degradation Pathways, Atrazine Mineralization and Metabolites Toxicity

The degradation of atrazine is a complex process with different pathways through different biotic or abiotic water treatment processes. Regarding the biotic degradation processes, there are two stages [146] (Figure 3). In the first stage, hydrolytic dichlorination and *N*-dealkylation of atrazine generate cyanuric acid in the role of the enzymes that have broad substrate specificity [147]. For hydrolytic dichlorination of atrazine, enzyme atrazine chlorohydrolase (AtzA) [148] or hydrolase triazine (TrzN) [149] catalyzes hydrolytic dichlorination of atrazine, but they display substantial differences in their substrate ranges: AtzA is restricted to atrazine analogs with a chlorine substituent at carbon 2 and *N*-alkyl groups, ranging in size from methyl to *t*-butyl [150], and TrzN hydrolyzes a range of leaving groups (e.g.,  $\text{OCH}_3$ ,  $-\text{SCH}_3$ ,  $-\text{Cl}$ ,  $-\text{F}$ ,  $-\text{CN}$ ) from both triazines and pyrimidines [149]. For *N*-dealkylation of atrazine, hydroxyatrazine *N*-ethylaminohydrolase (AtzB) [151] catalyzes the hydrolytic conversion of hydroxyatrazine to *N*-isopropylammelide, and *N*-isopropylammelide isopropylaminohydrolase (AtzC) [152] catalyzes the hydrolysis of *N*-isopropylammelide to cyanuric acid. In the second stage, cyanuric acid is converted to ammonium and carbon dioxide by a set of enzymes AtzDEF [153,154] and TrzD [153,155].

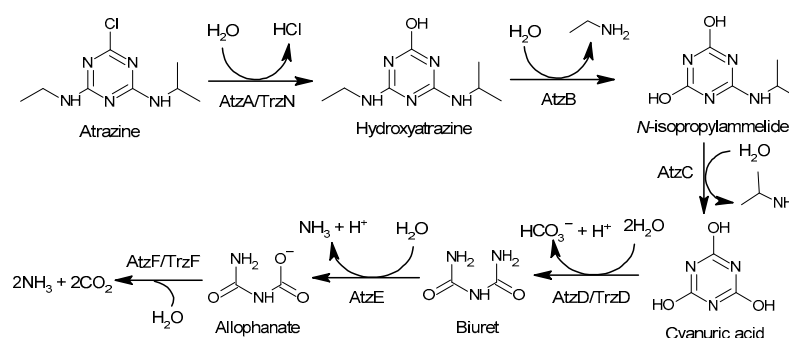


**Figure 3.** Degradation pathway of atrazine through biotic treatment process.

The above discussion is based on the enzymatic steps catalyzed by the gene products. In actual operation, atrazine degradation may be achieved by a consortium of organisms harboring the appropriate combination of enzymes, for example, the enriched mixed culture as well as the isolated strain, designated as *Arthrobacter* sp. strain GZK-1, mineralized  $^{14}\text{C}$ -ring-labeled atrazine up to 88% to  $^{14}\text{CO}_2$  in a liquid culture within 14 d [156].

In addition, for abiotic water treatment processes, as shown in Sections 2 and 3 of this article, many advanced oxidation processes (AOPs) have been involved in the degradation of atrazine in water. These AOPs can be used individually or in combination to improve efficiency such as US/UV [71,157], US/UV/O<sub>3</sub> [114,158], electrochemistry (EC)/O<sub>3</sub> [111], UV/H<sub>2</sub>O<sub>2</sub> [159], UV/US/PS [160], UV/MW [161,162], UV/Fenton [83], etc. Generally, AOPs rely on the in situ formation of reactive species [78], such as hydroxyl radical ( $\bullet\text{OH}$ ) [163], sulfate radical ( $\text{SO}_4^{\bullet-}$ ) [164,165], singlet oxygen ( $^1\text{O}_2$ ) [132], superoxide radical anions ( $\text{O}_2^{\bullet-}$ ) [37], hydrated electron ( $e_{\text{aq}}^-$ ) [78] and hydrogen radical ( $\text{H}\bullet$ ) [78]. These reactive species have different redox potential and reaction selectivity. Therefore, the degradation pathways of atrazine vary from different AOPs. The general involved mechanisms were de-chlorination, hydroxylation of the s-triazazine ring, de-alkylation of the amino groups, oxidation of the amino groups, de-amination and the opening of the s-triazazine ring [71] (Figure 4). In most previous works [71,92,114,132,165], the final products of atrazine degradation tend to be cyanuric acid, ammelide and ammeline, because it is difficult to cleave the s-triazazine ring [166]. At present, few studies [45,75,81,167,168] have reported the complete mineralization of atrazine, in which s-triazazine ring-cleavage produced the less toxic compound biuret [167], and biuret hydrolyzed to allophanate, followed by the final generation of  $\text{CO}_2$ ,  $\text{H}_2\text{O}$ ,  $\text{NH}_4^+$  and small acids. The complete mineralization of atrazine thus reduces the toxicity of the treated wastewater for subsequent release.

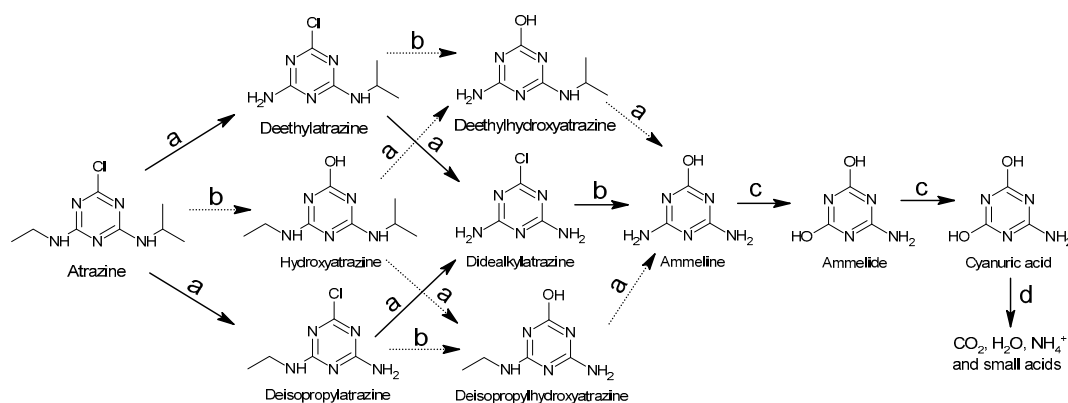


**Figure 4.** General involved degradation mechanisms of atrazine: (a) dealkylation of the amino groups; (b) dechlorination and hydroxylation of the s-triazazine ring; (c) oxidation of the amino groups and deamination; (d) the opening of the s-triazazine ring.

Toxicity studies on atrazine degradation are still incomplete, because some atrazine metabolites such as ammeline lack toxicological data. According to the book “Pesticide residues in food: 2007, toxicological evaluations”, published by the World Health Organization [169], atrazine, and its chloro-s-triazazine metabolites are of moderate or low acute oral toxicity in male rats ( $\text{LD}_{50}$ ), 1870–3090, 1890, 2290 and 3690 mg/kg bw for ATZ, DEA, DIA and DDA, respectively; and the acute oral toxicity of hydroxyatrazine in male rats ( $\text{LD}_{50}$ , >5050 mg/kg bw) is lower than that of atrazine or its chlorometabolites. However, toxicity comparisons based on these  $\text{LD}_{50}$  values are still inaccurate, as the results of toxicity tests vary based on different subjects (plants, animals, human cells, etc.) or different concerns (reproductive or developmental toxicity, liver toxicity, etc.). More toxicity tests data are shown above (Table 8). Combining these data, the following toxicity ranking can be roughly obtained: atrazine (ATZ) > deethylatrazine (DEA) > deisopropylatrazine (DIA) > ammeline (AM) > didealkylatrazine (DDA) > hydroxyatrazine (HA).

**Table 8.** Chemical structures and toxicity tests data of atrazine and its metabolites.

Name	Atrazine (ATZ)	Deeth-Ylatrazine (DEA)	Deisoprop-Ylatrazine (DIA)	Ammeline (AM)	Cyanuric Acid	Dideal-Kylatrazine (DDA)	Hydroxy-Atrazine (HA)
Chemical structure							
Acute oral toxicity in male rats (LD <sub>50</sub> ) [169]	1870–3090 mg/kg	1890 mg/kg	2290 mg/kg			3690 mg/kg	>5050 mg/kg
Median lethal concentrations (LC <sub>50</sub> ) for <i>Pseudokirchneriella subcapitata</i> in 96 h of exposure [170]	1600 µg/L	2000 µg/L	>3000 µg/L				
Concentration for 50% of maximal effect (EC <sub>50</sub> ) on algal photosynthesis for <i>A. variabilis</i> [171]	0.1 ppm	0.7 ppm	4.7 ppm			100 ppm	>100 ppm
Acute oral toxicity in rats (LD <sub>50</sub> ) [171]					>5000 mg/kg		
Adverse effects in sheep [172]				An average daily intake of ammeline 296 mg/kg body weight per day for 42 days for sheep caused half death.	No adverse effects at doses from 198 to 600 mg/kg body weight per day for 77 days.		

In addition, Banghai Liu et.al. [90] used the ECOSAR program to predict the acute and chronic toxicity of atrazine and its transformation intermediates, and it was found that although the vast majority of detected products possessed lower toxicity compared to atrazine, they remained classified as very toxic compounds to aquatic organisms.

The degradation mechanism, atrazine degradation rate, mineralization rate and main products are different for different treatment process. For better elaboration, the following discussion is based on treatment process type.

As Table A1 shows, generally, different methods can achieve high degradation rates (>90%) of atrazine by filtering the optimal conditions, but the treatment time needed and atrazine degrading capacity vary. Figure 5 is a comparison of treatment time and atrazine product distribution of different methods based on the data listed in Table A1. We can see that the processing time required for biodegradation is significantly more than other methods, while HVED and Fenton/Fenton-like method take less time (Figure 5a). In addition, ring cleavage can be achieved by microbial degradation as well as HVED (Figure 5b). Compared with the Fenton method, HVED has the advantages of short processing time, high atrazine degrading capacity and low toxic product distribution.

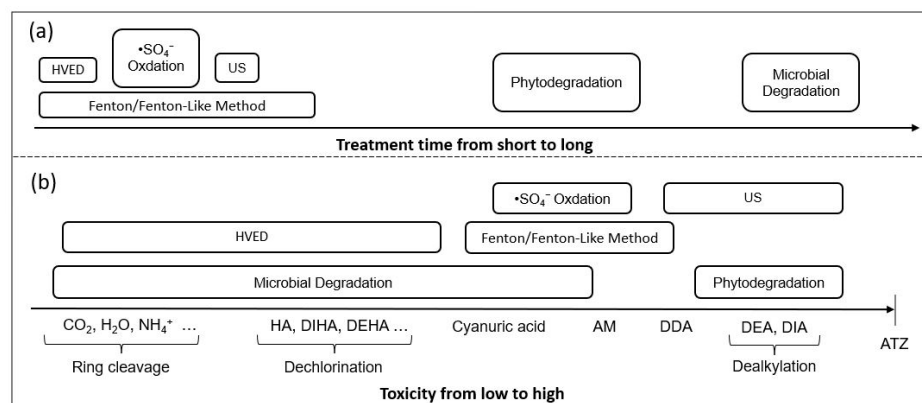


**Figure 5.** Comparison of different methods: (a) treatment time (b) product distribution.

## 6. Conclusions

As a widely used herbicide, atrazine is widely sprayed on many crops. Atrazine remaining in agri-food can cause physiological toxicity for a long time if it is ingested by humans. Additionally, because of chemical stability, atrazine in agri-food washing water flows into surface or groundwater and persists to be difficult to degrade. It is therefore of significant interest to develop clean and economical degradation processes for atrazine.

At present, biological processes are the common methods for the degradation of aqueous atrazine due to environmental protection, but biodegradation has its own limitations, such as slow degradation kinetics, and low remediation efficiency. Therefore, many studies have been focused on more highly efficient treatment technologies of aqueous atrazine, especially advanced oxidation processes (AOPs) that generate powerful nonspecific oxidant, hydroxyl radicals  $\cdot\text{OH}$ . Previous research reported the treatment of aqueous atrazine using  $\cdot\text{OH}$  generated by physicochemical methods and chemical methods. In these methods, a single technology processing or a co-processing of two or more technologies will be used, and often the latter can achieve a more ideal degradation rate. In addition to pursuing a high atrazine degradation rate, it is also significant to improve the degradation ability to achieve full mineralization. Therefore, more and more innovative technologies have been investigated, especially High Voltage Electrical Discharge (HVED). However, these new methods for the degradation of atrazine are still being explored, and further research is needed.

**Author Contributions:** Writing—original draft preparation, J.H.; writing—review and editing, J.H., N.B., G.E., F.M. and N.G.; supervision, F.M. and N.G.; project administration, F.M. and N.G. All authors have read and agreed to the published version of the manuscript.

**Funding:** This research received no external funding.

**Institutional Review Board Statement:** Not applicable.

**Informed Consent Statement:** Not applicable.

**Data Availability Statement:** Not applicable.

**Acknowledgments:** The first author would like to acknowledge financial support provided by the China Scholarship Council (CSC).

**Conflicts of Interest:** The authors declare no conflict of interest.

## Appendix A

Table A1. Comparison of different methods (degradation mechanism, atrazine degradation rate, atrazine mineralization rate and main products).

Method	Degradation Mechanism	Strain/Plant/Generated Reactive Species	Initial Atrazine Concentration and Some Notes	Treatment Time	Atrazine Degradation Rate	Atrazine Degrading Capacity	Products	References
Microbial Degradation	Microbes' express atrazine-degrading enzymes that degrade atrazine.	<i>Chelatobacter heintzii</i> Cit1	The initial atrazine concentration is 0.5 mg per kg of soil. The bacteria described were isolated from 12 cultivated and grassland soils from different areas in France.	131 days	No residual atrazine detected	Ring cleavage	CO <sub>2</sub> , H <sub>2</sub> O ...	[153]
		<i>Chelatobacter heintzii</i> Sal1-3						
		<i>Chelatobacter heintzii</i> LR3-3						
		<i>Chelatobacter heintzii</i> LRA						
		<i>Chelatobacter heintzii</i> SalB						
		<i>Chelatobacter heintzii</i> Lous2-3			56%	Dechlorination	Dechlorination products	
		<i>Chelatobacter heintzii</i> Sal2			No residual atrazine detected	Dechlorination	Dechlorination products	
		<i>Pseudomonas</i> sp. ADP				Ring cleavage	CO <sub>2</sub> , H <sub>2</sub> O ...	
<i>Arthrobacter cristallopoides</i> Cit2	Cyanuric acid production	Cyanuric acid						
<i>Nocardioides</i> sp. SP12								



Table A1. Cont.

Method	Degradation Mechanism	Strain/Plant/Generated Reactive Species	Initial Atrazine Concentration and Some Notes	Treatment Time	Atrazine Degradation Rate	Atrazine Degrading Capacity	Products	References
Phytodegradation	Phytoextraction: atrazine in soil and groundwater can be taken up inside plant tissues; Phytotransformation: atrazine inside plant tissues can be transformed by plant enzymes; Rhizoremediation: pollutants in soil can be degraded by microbes in the root zone.	Tall fescue Ryegrass Barley Maize	49 days after planting, the soils were spiked with aqueous solutions of atrazine to achieve concentrations of 2, 5 and 10 mg of atrazine per kg of soil. The plants were harvested after 65 days, that is, 16 days after atrazine application.	16 days	88.6–96.7%	Dealkylation	DIA and DEA	[173]
					96.6–99.6%			
					96.4–99.4%			
					97.2–98.6%			
Fenton/Fenton-like Method	H <sub>2</sub> O <sub>2</sub> reacts with Fe <sup>2+</sup> to generate reactive radicals •OH, which degrade atrazine.	•OH	The optimal mixture, 2.69 mM (1:1) FeSO <sub>4</sub> :H <sub>2</sub> O <sub>2</sub> , degraded [2,4,6- <sup>14</sup> C]-atrazine (140 μmol).	≤30 s	100%	Dealkylation	DDA	[174]
			The photo-Fenton process: 10 mg/L atrazine was degraded, using 1 g/L Heterogeneous Fenton catalyst Fe/TiO <sub>2</sub> , 1.6 mM H <sub>2</sub> O <sub>2</sub> and pH = 3. The light intensity at 420 nm was 30 W/m <sup>2</sup> .	30 min	95%	Ring cleavage (TOC removal rate 18%)	DDA, Cyanuric acid ...	[81]
			The initial concentration of atrazine was 23 μmol/L. The electro-Fenton process: the simultaneous reduction in ferric ions and oxygen at a simple electrode allowed the subsequent production of •OH.	4 h	100%	Dealkylation	DDA	[29]

Table A1. Cont.

Method	Degradation Mechanism	Strain/Plant/Generated Reactive Species	Initial Atrazine Concentration and Some Notes	Treatment Time	Atrazine Degradation Rate	Atrazine Degrading Capacity	Products	References
Sulfate Radical (SO <sub>4</sub> <sup>•-</sup> ) Oxidation	With the activation of persulfate (PS), sulfate radical (SO <sub>4</sub> <sup>•-</sup> ) can be generated by the cleavage of O–O bond of PS. Meanwhile, SO <sub>4</sub> <sup>•-</sup> could react with water and OH <sup>-</sup> to produce hydroxyl radicals (•OH).	SO <sub>4</sub> <sup>•-</sup> and •OH	The initial concentration of atrazine was 50 µmol/L. Copper sulfide (CuS)/ persulfate (PS)	40 min	91.6%	Dealkylation and Dechlorination	AM	[93]
			The initial concentration of atrazine was 10 mmol/L. Magnetite Fe <sub>3</sub> O <sub>4</sub> -sepiolite/ persulfate (PS)	1 h	72.3%			[95]
			The initial concentration of atrazine was 20 mg/L. Pyrite (FeS <sub>2</sub> ) / persulfate (PS)	45 min	100 %			[37]
High Voltage Electrical Discharges (HVED)	HVED can not only generate radical species, such as •OH, HO <sub>2</sub> <sup>•</sup> , and H <sup>•</sup> , ions, and free electrons (e <sup>-</sup> ), but also generate physical agents, such as UV, shock waves, and heat.	•OH	The initial concentration of atrazine was 11.9 mg/L. Dielectric barrier discharge (DBD)	18 min	93.7%	Ring cleavage (TOC removal rate 12.7%)	Dechlorination products, CO <sub>2</sub> , H <sub>2</sub> O ...	[67]
Ultrasound (US)	The high energy generated by the collapse of the ultrasonic cavitation bubble leads to the generation of hydroxyl radicals (•OH) and hydrogen radicals (•H).	•OH	The initial concentration of atrazine was 0.1 mmol/L. Ultrasound frequency: 500 kHz	80 min	100%	Dealkylation	DEA, DIA, DDA	[70]

## References

1. Udiković-Kolić, N.; Scott, C.; Martin-Laurent, F. Evolution of atrazine-degrading capabilities in the environment. *Appl. Microbiol. Biotechnol.* **2012**, *96*, 1175–1189. [[CrossRef](#)] [[PubMed](#)]
2. Fan, X.; Song, F. Bioremediation of atrazine: Recent advances and promises. *J. Soils Sediments* **2014**, *14*, 1727–1737. [[CrossRef](#)]
3. He, H.; Liu, Y.; You, S.; Liu, J.; Xiao, H.; Tu, Z. A Review on Recent Treatment Technology for Herbicide Atrazine in Contaminated Environment. *Int. J. Environ. Res. Public Health* **2019**, *16*, 5129. [[CrossRef](#)]
4. Komang Ralebitso, T.; Senior, E.; van Verseveld, H.W. Microbial aspects of atrazine degradation in natural environments. *Biodegradation* **2002**, *13*, 11–19. [[CrossRef](#)] [[PubMed](#)]
5. Chandra, P.N.; Usha, K. Removal of atrazine herbicide from water by polyelectrolyte multilayer membranes. *Mater. Today Proc.* **2021**, *41*, 622–627. [[CrossRef](#)]
6. European Food Safety, A. Reasoned opinion on the setting of a new maximum residue level for atrazine in cereals. *EFSA J.* **2015**, *13*, 4126. [[CrossRef](#)]
7. Wirbisky, S.E.; Freeman, J.L. Atrazine Exposure and Reproductive Dysfunction through the Hypothalamus-Pituitary-Gonadal (HPG) Axis. *Toxics* **2015**, *3*, 414. [[CrossRef](#)]
8. Hayes, T.B.; Khoury, V.; Narayan, A.; Nazir, M.; Park, A.; Brown, T.; Adame, L.; Chan, E.; Buchholz, D.; Stueve, T.; et al. Atrazine induces complete feminization and chemical castration in male African clawed frogs (*Xenopus laevis*). *Proc. Natl. Acad. Sci. USA* **2010**, *107*, 4612. [[CrossRef](#)]
9. Pathak, R.K.; Dikshit, A.K. Atrazine and Human Health. *Int. J. Ecosyst.* **2011**, *1*, 14–23. [[CrossRef](#)]
10. Bethsass, J.; Colangelo, A. European Union Bans Atrazine, While the United States Negotiates Continued Use. *Int. J. Occup. Environ. Health* **2006**, *12*, 260–267. [[CrossRef](#)]
11. Farruggia, F.T.; Rossmel, C.M.; Hetrick, J.A.; Biscoe, M.; Branch, M., III. *Refined Ecological Risk Assessment for Atrazine*; US Environmental Protection Agency, Office of Pesticide Programs: Washington, DC, USA, 2016.
12. Esteves, R.C.; do Amaral Vendramini, A.L.; Accioly, F. A qualitative meta-synthesis study of the convergence between organic crop regulations in the United States, Brazil, and Europe. *Trends Food Sci. Technol.* **2021**, *107*, 343–357. [[CrossRef](#)]
13. Megiato, E.I.; Massuquetti, A.; de Azevedo, A.F.Z. Impacts of integration of Brazil with the European Union through a general equilibrium model. *Economia* **2016**, *17*, 126–140. [[CrossRef](#)]
14. Wu, S.; Li, H.; Li, X.; He, H.; Yang, C. Performances and mechanisms of efficient degradation of atrazine using peroxymonosulfate and ferrate as oxidants. *Chem. Eng. J.* **2018**, *353*, 533–541. [[CrossRef](#)]
15. Khan, S.U.; Saidak, W.J. Residues of atrazine and its metabolites after prolonged usage. *Weed Res.* **1981**, *21*, 9–12. [[CrossRef](#)]
16. James, T.K.; Ghanizadeh, H.; Harrington, K.C.; Bolan, N.S. Degradation of atrazine and bromacil in two forestry waste products. *Sci. Rep.* **2021**, *11*, 3284. [[CrossRef](#)]
17. Wauchope, R.D.; Buttler, T.M.; Hornsby, A.G.; Augustijn-Beckers, P.W.M.; Burt, J.P. The SCS/ARS/CES Pesticide Properties Database for Environmental Decision-Making. In *Reviews of Environmental Contamination and Toxicology: Continuation of Residue Reviews*; Ware, G.W., Ed.; Springer: New York, NY, USA, 1992; pp. 1–155.
18. Balci, B.; Oturan, N.; Cherrier, R.; Oturan, M.A. Degradation of atrazine in aqueous medium by electrocatalytically generated hydroxyl radicals. A kinetic and mechanistic study. *Water Res.* **2009**, *43*, 1924–1934. [[CrossRef](#)]
19. Belluck, D.A.; Benjamin, S.L.; Dawson, T. Groundwater Contamination by Atrazine and Its Metabolites. In *Pesticide Transformation Products*; ACS Symposium Series; American Chemical Society: Washington, DC, USA, 1991; Volume 459, pp. 254–273.
20. Mahía, J.; Martín, A.; Carballas, T.; Díaz-Raviña, M. Atrazine degradation and enzyme activities in an agricultural soil under two tillage systems. *Sci. Total Environ.* **2007**, *378*, 187–194. [[CrossRef](#)]
21. Bohn, T.; Cocco, E.; Gourdol, L.; Guignard, C.; Hoffmann, L. Determination of atrazine and degradation products in Luxembourgish drinking water: Origin and fate of potential endocrine-disrupting pesticides. *Food Addit. Contam. Part A* **2011**, *28*, 1041–1054. [[CrossRef](#)]
22. Pereira, W.E.; Rostad, C.E. Occurrence, distributions, and transport of herbicides and their degradation products in the Lower Mississippi River and its tributaries. *Environ. Sci. Technol.* **1990**, *24*, 1400–1406. [[CrossRef](#)]
23. Yan, D.-h.; He, Y.; Wang, H. Environmental characteristics of the atrazine in the waters in East Liaohe River Basin. *Huan Jing Ke Xue* **2005**, *26*, 203–208. (In Chinese) [[PubMed](#)]
24. Antić, N.; Radišić, M.; Radović, T.; Vasiljević, T.; Grujić, S.; Petković, A.; Dimkić, M.; Laušević, M. Pesticide Residues in the Danube River Basin in Serbia—A Survey during 2009–2011. *CLEAN Soil Air Water* **2015**, *43*, 197–204. [[CrossRef](#)]
25. Steffens, C.; Ballen, S.C.; Scapin, E.; da Silva, D.M.; Steffens, J.; Jacques, R.A. Advances of nanobiosensors and its application in atrazine detection in water: A review. *Sens. Actuators Rep.* **2022**, *4*, 100096. [[CrossRef](#)]
26. Salahshoor, Z.; Ho, K.-V.; Hsu, S.-Y.; Lin, C.-H.; Fidalgo de Cortalezzi, M. Detection of Atrazine and its metabolites by photonic molecularly imprinted polymers in aqueous solutions. *Chem. Eng. J. Adv.* **2022**, *12*, 100368. [[CrossRef](#)]
27. Farooq, S.; Wu, H.; Nie, J.; Ahmad, S.; Muhammad, L.; Zeeshan, M.; Khan, R.; Asim, M. Application, advancement and green aspects of magnetic molecularly imprinted polymers in pesticide residue detection. *Sci. Total Environ.* **2022**, *804*, 150293. [[CrossRef](#)] [[PubMed](#)]
28. Farooq, S.; Nie, J.; Cheng, Y.; Yan, Z.; Li, J.; Bacha, S.A.S.; Mushtaq, A.; Zhang, H. Molecularly imprinted polymers' application in pesticide residue detection. *Analyst* **2018**, *143*, 3971–3989. [[CrossRef](#)]

29. Ventura, A.; Jacquet, G.; Bermond, A.; Camel, V. Electrochemical generation of the Fenton's reagent: Application to atrazine degradation. *Water Res.* **2002**, *36*, 3517–3522. [[CrossRef](#)]
30. Saltmiras, D.A.; Lemley, A.T. Atrazine degradation by anodic Fenton treatment. *Water Res.* **2002**, *36*, 5113–5119. [[CrossRef](#)]
31. Chu, W.; Chan, K.H.; Kwan, C.Y.; Choi, K.Y. Degradation of atrazine by modified stepwise-Fenton's processes. *Chemosphere* **2007**, *67*, 755–761. [[CrossRef](#)] [[PubMed](#)]
32. Du, Y.; Zhao, L.; Su, Y. Tantalum (oxy)nitrides: Preparation, characterisation and enhancement of photo-Fenton-like degradation of atrazine under visible light. *J. Hazard. Mater.* **2011**, *195*, 291–297. [[CrossRef](#)] [[PubMed](#)]
33. Du, Y.; Zhao, L.; Chang, Y.; Su, Y. Tantalum (oxy)nitrides nanotube arrays for the degradation of atrazine in vis-Fenton-like process. *J. Hazard. Mater.* **2012**, *225–226*, 21–27. [[CrossRef](#)] [[PubMed](#)]
34. Jiang, Q.; Zhang, Y.; Jiang, S.; Wang, Y.; Li, H.; Han, W.; Qu, J.; Wang, L.; Hu, Y. Graphene-like carbon sheet-supported nZVI for efficient atrazine oxidation degradation by persulfate activation. *Chem. Eng. J.* **2021**, *403*, 126309. [[CrossRef](#)]
35. Zhang, Y.; Jiang, Q.; Jiang, S.; Li, H.; Zhang, R.; Qu, J.; Zhang, S.; Han, W. One-step synthesis of biochar supported nZVI composites for highly efficient activating persulfate to oxidatively degrade atrazine. *Chem. Eng. J.* **2021**, *420*, 129868. [[CrossRef](#)]
36. Li, G.; Guo, Y.; Jin, Y.; Tan, W.; Liu, F.; Yin, H. Intrinsic mechanisms of calcium sulfite activation by siderite for atrazine degradation. *Chem. Eng. J.* **2021**, *426*, 131917. [[CrossRef](#)]
37. Wang, X.; Wang, Y.; Chen, N.; Shi, Y.; Zhang, L. Pyrite enables persulfate activation for efficient atrazine degradation. *Chemosphere* **2020**, *244*, 125568. [[CrossRef](#)]
38. Deng, S.; Liu, L.; Cagnetta, G.; Huang, J.; Yu, G. Mechanochemically synthesized S-ZVIbm composites for the activation of persulfate in the pH-independent degradation of atrazine: Effects of sulfur dose and ball-milling conditions. *Chem. Eng. J.* **2021**, *423*, 129789. [[CrossRef](#)]
39. Khavar, A.H.C.; Moussavi, G.; Mahjoub, A.R.; Satari, M.; Abdolmaleki, P. Synthesis and visible-light photocatalytic activity of In,S-TiO<sub>2</sub>@rGO nanocomposite for degradation and detoxification of pesticide atrazine in water. *Chem. Eng. J.* **2018**, *345*, 300–311. [[CrossRef](#)]
40. Wang, W.-K.; Chen, J.-J.; Gao, M.; Huang, Y.-X.; Zhang, X.; Yu, H.-Q. Photocatalytic degradation of atrazine by boron-doped TiO<sub>2</sub> with a tunable rutile/anatase ratio. *Appl. Catal. B Environ.* **2016**, *195*, 69–76. [[CrossRef](#)]
41. Granados-Oliveros, G.; Páez-Mozo, E.A.; Ortega, F.M.; Ferronato, C.; Chovelon, J.-M. Degradation of atrazine using metalloporphyrins supported on TiO<sub>2</sub> under visible light irradiation. *Appl. Catal. B Environ.* **2009**, *89*, 448–454. [[CrossRef](#)]
42. Zhang, Y.; Han, C.; Zhang, G.; Dionysiou, D.D.; Nadagouda, M.N. PEG-assisted synthesis of crystal TiO<sub>2</sub> nanowires with high specific surface area for enhanced photocatalytic degradation of atrazine. *Chem. Eng. J.* **2015**, *268*, 170–179. [[CrossRef](#)]
43. Yola, M.L.; Eren, T.; Atar, N. A novel efficient photocatalyst based on TiO<sub>2</sub> nanoparticles involved boron enrichment waste for photocatalytic degradation of atrazine. *Chem. Eng. J.* **2014**, *250*, 288–294. [[CrossRef](#)]
44. Chen, S.; He, P.; Wang, X.; Xiao, F.; Zhou, P.; He, Q.; Jia, L.; Dong, F.; Zhang, H.; Jia, B.; et al. Co/Sm-modified Ti/PbO<sub>2</sub> anode for atrazine degradation: Effective electrocatalytic performance and degradation mechanism. *Chemosphere* **2021**, *268*, 128799. [[CrossRef](#)] [[PubMed](#)]
45. Teng, X.; Li, J.; Wang, J.; Liu, J.; Ge, X.; Gu, T. Effective degradation of atrazine in wastewater by three-dimensional electrochemical system using fly ash-red mud particle electrode: Mechanism and pathway. *Sep. Purif. Technol.* **2021**, *267*, 118661. [[CrossRef](#)]
46. Sun, X.; Qi, H.; Sun, Z. Bifunctional nickel foam composite cathode co-modified with CoFe@NC and CNTs for electrocatalytic degradation of atrazine over wide pH range. *Chemosphere* **2022**, *286*, 131972. [[CrossRef](#)]
47. Wang, T.; Huang, T.; Jiang, H.; Ma, R. Electrochemical degradation of atrazine by BDD anode: Evidence from compound-specific stable isotope analysis and DFT simulations. *Chemosphere* **2021**, *273*, 129754. [[CrossRef](#)]
48. McBeath, S.T.; Graham, N.J.D. In-situ electrochemical generation of permanganate for the treatment of atrazine. *Sep. Purif. Technol.* **2021**, *260*, 118252. [[CrossRef](#)]
49. Ma, J.; Graham, N.J.D. Degradation of atrazine by manganese-catalysed ozonation: Influence of humic substances. *Water Res.* **1999**, *33*, 785–793. [[CrossRef](#)]
50. Chu, W.; Chan, K.H.; Graham, N.J.D. Enhancement of ozone oxidation and its associated processes in the presence of surfactant: Degradation of atrazine. *Chemosphere* **2006**, *64*, 931–936. [[CrossRef](#)]
51. Yuan, X.; Yan, X.; Xu, H.; Li, D.; Sun, L.; Cao, G.; Xia, D. Enhanced ozonation degradation of atrazine in the presence of nano-ZnO: Performance, kinetics and effects. *J. Environ. Sci.* **2017**, *61*, 3–13. [[CrossRef](#)] [[PubMed](#)]
52. Zhu, S.; Dong, B.; Yu, Y.; Bu, L.; Deng, J.; Zhou, S. Heterogeneous catalysis of ozone using ordered mesoporous Fe<sub>3</sub>O<sub>4</sub> for degradation of atrazine. *Chem. Eng. J.* **2017**, *328*, 527–535. [[CrossRef](#)]
53. Yang, J.; Li, J.; Dong, W.; Ma, J.; Cao, J.; Li, T.; Li, J.; Gu, J.; Liu, P. Study on enhanced degradation of atrazine by ozonation in the presence of hydroxylamine. *J. Hazard. Mater.* **2016**, *316*, 110–121. [[CrossRef](#)]
54. Zhang, Y.; Jiang, Z.; Cao, B.; Hu, M.; Wang, Z.; Dong, X. Metabolic ability and gene characteristics of *Arthrobacter* sp. strain DNS10, the sole atrazine-degrading strain in a consortium isolated from black soil. *Int. Biodeterior. Biodegrad.* **2011**, *65*, 1140–1144. [[CrossRef](#)]
55. Jiang, Z.; Chen, J.; Li, J.; Cao, B.; Chen, Y.; Liu, D.; Wang, X.; Zhang, Y. Exogenous Zn<sup>2+</sup> enhance the biodegradation of atrazine by regulating the chlorohydrolase gene *trzN* transcription and membrane permeability of the degrader *Arthrobacter* sp. DNS10. *Chemosphere* **2020**, *238*, 124594. [[CrossRef](#)] [[PubMed](#)]

56. Khatoon, H.; Rai, J.P.N. Optimization studies on biodegradation of atrazine by *Bacillus badius* ABP6 strain using response surface methodology. *Biotechnol. Rep.* **2020**, *26*, e00459. [[CrossRef](#)] [[PubMed](#)]
57. Dhiman, N.; Jasrotia, T.; Sharma, P.; Negi, S.; Chaudhary, S.; Kumar, R.; Mahnashi, M.H.; Umar, A.; Kumar, R. Immobilization interaction between xenobiotic and *Bjerkandera adusta* for the biodegradation of atrazine. *Chemosphere* **2020**, *257*, 127060. [[CrossRef](#)]
58. Yu, T.; Wang, L.; Ma, F.; Wang, Y.; Bai, S. A bio-functions integration microcosm: Self-immobilized biochar-pellets combined with two strains of bacteria to remove atrazine in water and mechanisms. *J. Hazard. Mater.* **2020**, *384*, 121326. [[CrossRef](#)]
59. Singh, N.; Megharaj, M.; Kookana, R.S.; Naidu, R.; Sethunathan, N. Atrazine and simazine degradation in Pennisetum rhizosphere. *Chemosphere* **2004**, *56*, 257–263. [[CrossRef](#)]
60. Zhang, J.J.; Lu, Y.C.; Yang, H. Chemical Modification and Degradation of Atrazine in *Medicago sativa* through Multiple Pathways. *J. Agric. Food Chem.* **2014**, *62*, 9657–9668. [[CrossRef](#)]
61. Lu, Y.C.; Feng, S.J.; Zhang, J.J.; Luo, F.; Zhang, S.; Yang, H. Genome-wide identification of DNA methylation provides insights into the association of gene expression in rice exposed to pesticide atrazine. *Sci. Rep.* **2016**, *6*, 18985. [[CrossRef](#)]
62. Lu, Y.C.; Luo, F.; Pu, Z.J.; Zhang, S.; Huang, M.T.; Yang, H. Enhanced detoxification and degradation of herbicide atrazine by a group of *O*-methyltransferases in rice. *Chemosphere* **2016**, *165*, 487–496. [[CrossRef](#)]
63. Zhang, J.J.; Lu, Y.C.; Zhang, S.H.; Lu, F.F.; Yang, H. Identification of transcriptome involved in atrazine detoxification and degradation in alfalfa (*Medicago sativa*) exposed to realistic environmental contamination. *Ecotoxicol. Environ. Saf.* **2016**, *130*, 103–112. [[CrossRef](#)]
64. Hoeben, W.; Van Veldhuizen, E.; Classens, H.; Rutgers, W. The Degradation of Phenol and Atrazine in Water by Pulsed Corona Discharges. In Proceedings of the 13th International Symposium on Plasma Chemistry, Beijing, China, 18–22 August 1997; pp. 18–22.
65. Karpel Vel Leitner, N.; Syoen, G.; Romat, H.; Urashima, K.; Chang, J.S. Generation of active entities by the pulsed arc electrohydraulic discharge system and application to removal of atrazine. *Water Res.* **2005**, *39*, 4705–4714. [[CrossRef](#)] [[PubMed](#)]
66. Mededovic, S.; Locke, B.R. Side-Chain Degradation of Atrazine by Pulsed Electrical Discharge in Water. *Ind. Eng. Chem. Res.* **2007**, *46*, 2702–2709. [[CrossRef](#)]
67. Zhu, D.; Jiang, L.; Liu, R.-l.; Chen, P.; Lang, L.; Feng, J.-w.; Yuan, S.-j.; Zhao, D.-y. Wire-cylinder dielectric barrier discharge induced degradation of aqueous atrazine. *Chemosphere* **2014**, *117*, 506–514. [[CrossRef](#)] [[PubMed](#)]
68. Vanraes, P.; Willems, G.; Daels, N.; Van Hulle, S.W.H.; De Clerck, K.; Surmont, P.; Lynen, F.; Vandamme, J.; Van Durme, J.; Nikiforov, A.; et al. Decomposition of atrazine traces in water by combination of non-thermal electrical discharge and adsorption on nanofiber membrane. *Water Res.* **2015**, *72*, 361–371. [[CrossRef](#)]
69. Vanraes, P.; Willems, G.; Nikiforov, A.; Surmont, P.; Lynen, F.; Vandamme, J.; Van Durme, J.; Verheust, Y.P.; Van Hulle, S.W.H.; Dumoulin, A.; et al. Removal of atrazine in water by combination of activated carbon and dielectric barrier discharge. *J. Hazard. Mater.* **2015**, *299*, 647–655. [[CrossRef](#)]
70. Petrier, C.; David, B.; Laguian, S. Ultrasonic degradation at 20 kHz and 500 kHz of atrazine and pentachlorophenol in aqueous solution: Preliminary results. *Chemosphere* **1996**, *32*, 1709–1718. [[CrossRef](#)]
71. Xu, L.J.; Chu, W.; Graham, N. Atrazine degradation using chemical-free process of USUV: Analysis of the micro-heterogeneous environments and the degradation mechanisms. *J. Hazard. Mater.* **2014**, *275*, 166–174. [[CrossRef](#)]
72. Jing, L.; Chen, B.; Wen, D.; Zheng, J.; Zhang, B. Pilot-scale treatment of atrazine production wastewater by UV/O<sub>3</sub>/ultrasound: Factor effects and system optimization. *J. Environ. Manag.* **2017**, *203*, 182–190. [[CrossRef](#)]
73. Xiong, G.; Liang, J.; Zou, S.; Zhang, Z. Microwave-assisted extraction of atrazine from soil followed by rapid detection using commercial ELISA kit. *Anal. Chim. Acta* **1998**, *371*, 97–103. [[CrossRef](#)]
74. Ta, N.; Hong, J.; Liu, T.; Sun, C. Degradation of atrazine by microwave-assisted electrodeless discharge mercury lamp in aqueous solution. *J. Hazard. Mater.* **2006**, *138*, 187–194. [[CrossRef](#)]
75. Zhanqi, G.; Shaogui, Y.; Na, T.; Cheng, S. Microwave assisted rapid and complete degradation of atrazine using TiO<sub>2</sub> nanotube photocatalyst suspensions. *J. Hazard. Mater.* **2007**, *145*, 424–430. [[CrossRef](#)] [[PubMed](#)]
76. Basfar, A.A.; Mohamed, K.A.; Al-Abdul, A.J.; Al-Shahrani, A.A. Radiolytic degradation of atrazine aqueous solution containing humic substances. *Ecotoxicol. Environ. Saf.* **2009**, *72*, 948–953. [[CrossRef](#)]
77. Mohamed, K.A.; Basfar, A.A.; Al-Shahrani, A.A. Gamma-ray induced degradation of diazinon and atrazine in natural groundwaters. *J. Hazard. Mater.* **2009**, *166*, 810–814. [[CrossRef](#)]
78. Khan, J.A.; Shah, N.S.; Nawaz, S.; Ismail, M.; Rehman, F.; Khan, H.M. Role of e<sub>aq</sub><sup>-</sup>, ·OH and H· in radiolytic degradation of atrazine: A kinetic and mechanistic approach. *J. Hazard. Mater.* **2015**, *288*, 147–157. [[CrossRef](#)] [[PubMed](#)]
79. Poonia, K.; Hasija, V.; Singh, P.; Parwaz Khan, A.A.; Thakur, S.; Thakur, V.K.; Mukherjee, S.; Ahamad, T.; Alshehri, S.M.; Raizada, P. Photocatalytic degradation aspects of atrazine in water: Enhancement strategies and mechanistic insights. *J. Clean. Prod.* **2022**, *367*, 133087. [[CrossRef](#)]
80. Rostami, S.; Jafari, S.; Moeini, Z.; Jaskulak, M.; Keshtgar, L.; Badeenezhad, A.; Azhdarpoor, A.; Rostami, M.; Zorena, K.; Dehghani, M. Current methods and technologies for degradation of atrazine in contaminated soil and water: A review. *Environ. Technol. Innov.* **2021**, *24*, 102019. [[CrossRef](#)]
81. Yang, N.; Liu, Y.; Zhu, J.; Wang, Z.; Li, J. Study on the efficacy and mechanism of Fe-TiO<sub>2</sub> visible heterogeneous Fenton catalytic degradation of atrazine. *Chemosphere* **2020**, *252*, 126333. [[CrossRef](#)]

82. Shi, Y.; Wang, X.; Liu, X.; Ling, C.; Shen, W.; Zhang, L. Visible light promoted Fe<sub>3</sub>S<sub>4</sub> Fenton oxidation of atrazine. *Appl. Catal. B Environ.* **2020**, *277*, 119229. [[CrossRef](#)]
83. Fareed, A.; Hussain, A.; Nawaz, M.; Imran, M.; Ali, Z.; Haq, S.U. The impact of prolonged use and oxidative degradation of Atrazine by Fenton and photo-Fenton processes. *Environ. Technol. Innov.* **2021**, *24*, 101840. [[CrossRef](#)]
84. Benzaquén, T.B.; Cuello, N.I.; Alfano, O.M.; Eimer, G.A. Degradation of Atrazine over a heterogeneous photo-fenton process with iron modified MCM-41 materials. *Catal. Today* **2017**, *296*, 51–58. [[CrossRef](#)]
85. Du, Y.; Zhao, L.; Zhang, Y. Roles of TaON and Ta<sub>3</sub>N<sub>5</sub> in the visible-Fenton-like degradation of atrazine. *J. Hazard. Mater.* **2014**, *267*, 55–61. [[CrossRef](#)] [[PubMed](#)]
86. Zhang, Y.; Du, Y.; Liu, D.; Bian, W. The role of dissolved oxygen in the Ta(O)N-driven visible Fenton-like degradation of atrazine. *J. Environ. Chem. Eng.* **2014**, *2*, 1691–1698. [[CrossRef](#)]
87. Wang, G.; Cheng, C.; Zhu, J.; Wang, L.; Gao, S.; Xia, X. Enhanced degradation of atrazine by nanoscale LaFe<sub>1-x</sub>Cu<sub>x</sub>O<sub>3-δ</sub> perovskite activated peroxymonosulfate: Performance and mechanism. *Sci. Total Environ.* **2019**, *673*, 565–575. [[CrossRef](#)]
88. Wu, S.; He, H.; Li, X.; Yang, C.; Zeng, G.; Wu, B.; He, S.; Lu, L. Insights into atrazine degradation by persulfate activation using composite of nanoscale zero-valent iron and graphene: Performances and mechanisms. *Chem. Eng. J.* **2018**, *341*, 126–136. [[CrossRef](#)]
89. Li, C.; Huang, Y.; Dong, X.; Sun, Z.; Duan, X.; Ren, B.; Zheng, S.; Dionysiou, D.D. Highly efficient activation of peroxymonosulfate by natural negatively-charged kaolinite with abundant hydroxyl groups for the degradation of atrazine. *Appl. Catal. B Environ.* **2019**, *247*, 10–23. [[CrossRef](#)]
90. Liu, B.; Guo, W.; Wang, H.; Si, Q.; Zhao, Q.; Luo, H.; Ren, N. Activation of peroxymonosulfate by cobalt-impregnated biochar for atrazine degradation: The pivotal roles of persistent free radicals and ecotoxicity assessment. *J. Hazard. Mater.* **2020**, *398*, 122768. [[CrossRef](#)]
91. Zhu, J.; Wang, J.; Shan, C.; Zhang, J.; Lv, L.; Pan, B. Durable activation of peroxymonosulfate mediated by Co-doped mesoporous FePO<sub>4</sub> via charge redistribution for atrazine degradation. *Chem. Eng. J.* **2019**, *375*, 122009. [[CrossRef](#)]
92. Zhang, R.; Wan, Y.; Peng, J.; Yao, G.; Zhang, Y.; Lai, B. Efficient degradation of atrazine by LaCoO<sub>3</sub>/Al<sub>2</sub>O<sub>3</sub> catalyzed peroxymonosulfate: Performance, degradation intermediates and mechanism. *Chem. Eng. J.* **2019**, *372*, 796–808. [[CrossRef](#)]
93. Peng, J.; Lu, X.; Jiang, X.; Zhang, Y.; Chen, Q.; Lai, B.; Yao, G. Degradation of atrazine by persulfate activation with copper sulfide (CuS): Kinetics study, degradation pathways and mechanism. *Chem. Eng. J.* **2018**, *354*, 740–752. [[CrossRef](#)]
94. Zhang, H.; Liu, X.; Lin, C.; Li, X.; Zhou, Z.; Fan, G.; Ma, J. Peroxymonosulfate activation by hydroxylamine-drinking water treatment residuals for the degradation of atrazine. *Chemosphere* **2019**, *224*, 689–697. [[CrossRef](#)]
95. Xu, X.; Chen, W.; Zong, S.; Ren, X.; Liu, D. Atrazine degradation using Fe<sub>3</sub>O<sub>4</sub>-sepiolite catalyzed persulfate: Reactivity, mechanism and stability. *J. Hazard. Mater.* **2019**, *377*, 62–69. [[CrossRef](#)] [[PubMed](#)]
96. Hong, Y.; Peng, J.; Zhao, X.; Yan, Y.; Lai, B.; Yao, G. Efficient degradation of atrazine by CoMgAl layered double oxides catalyzed peroxymonosulfate: Optimization, degradation pathways and mechanism. *Chem. Eng. J.* **2019**, *370*, 354–363. [[CrossRef](#)]
97. Huang, Y.; Han, C.; Liu, Y.; Nadagouda, M.N.; Machala, L.; O’Shea, K.E.; Sharma, V.K.; Dionysiou, D.D. Degradation of atrazine by Zn<sub>x</sub>Cu<sub>1-x</sub>Fe<sub>2</sub>O<sub>4</sub> nanomaterial-catalyzed sulfite under UV-vis light irradiation: Green strategy to generate SO<sub>4</sub><sup>-</sup>. *Appl. Catal. B Environ.* **2018**, *221*, 380–392. [[CrossRef](#)]
98. Popova, S.; Matafonova, G.; Batoev, V. Simultaneous atrazine degradation and E. coli inactivation by UV/S<sub>2</sub>O<sub>8</sub><sup>2-</sup>/Fe<sup>2+</sup> process under KrCl excilamp (222 nm) irradiation. *Ecotoxicol. Environ. Saf.* **2019**, *169*, 169–177. [[CrossRef](#)] [[PubMed](#)]
99. Noah, N. Chapter 6—Green synthesis: Characterization and application of silver and gold nanoparticles. In *Green Synthesis, Characterization and Applications of Nanoparticles*; Shukla, A.K., Irvani, S., Eds.; Elsevier: Amsterdam, The Netherlands, 2019; pp. 111–135.
100. Fernández-Domene, R.M.; Sánchez-Tovar, R.; Lucas-granados, B.; Muñoz-Portero, M.J.; García-Antón, J. Elimination of pesticide atrazine by photoelectrocatalysis using a photoanode based on WO<sub>3</sub> nanosheets. *Chem. Eng. J.* **2018**, *350*, 1114–1124. [[CrossRef](#)]
101. Xie, S.; Tang, C.; Shi, H.; Zhao, G. Highly efficient photoelectrochemical removal of atrazine and the mechanism investigation: Bias potential effect and reactive species. *J. Hazard. Mater.* **2021**, *415*, 125681. [[CrossRef](#)]
102. Gondal, M.A.; Suliman, M.A.; Dastageer, M.A.; Chuah, G.-K.; Basheer, C.; Yang, D.; Suwaiyan, A. Visible light photocatalytic degradation of herbicide (Atrazine) using surface plasmon resonance induced in mesoporous Ag-WO<sub>3</sub>/SBA-15 composite. *J. Mol. Catal. A Chem.* **2016**, *425*, 208–216. [[CrossRef](#)]
103. Mahlalela, L.C.; Casado, C.; Marugán, J.; Septien, S.; Ndlovu, T.; Dlamini, L.N. Synthesis of platelet-like BiVO<sub>4</sub> using hyperbranched polyethyleneimine for the formation of heterojunctions with Bi<sub>2</sub>O<sub>3</sub>. *Appl. Nanosci.* **2019**, *9*, 1501–1514. [[CrossRef](#)]
104. Mahlalela, L.C.; Casado, C.; Marugán, J.; Septien, S.; Ndlovu, T.; Dlamini, L.N. Photocatalytic degradation of atrazine in aqueous solution using hyperbranched polyethyleneimine templated morphologies of BiVO<sub>4</sub> fused with Bi<sub>2</sub>O<sub>3</sub>. *J. Environ. Chem. Eng.* **2020**, *8*, 104215. [[CrossRef](#)]
105. Majhi, D.; Das, K.; Mishra, A.; Dhiman, R.; Mishra, B.G. One pot synthesis of CdS/BiOBr/Bi<sub>2</sub>O<sub>2</sub>CO<sub>3</sub>: A novel ternary double Z-scheme heterostructure photocatalyst for efficient degradation of atrazine. *Appl. Catal. B Environ.* **2020**, *260*, 118222. [[CrossRef](#)]
106. Xue, Y.; Wang, P.; Wang, C.; Ao, Y. Efficient degradation of atrazine by BiOBr/UiO-66 composite photocatalyst under visible light irradiation: Environmental factors, mechanisms and degradation pathways. *Chemosphere* **2018**, *203*, 497–505. [[CrossRef](#)] [[PubMed](#)]

107. Moyet, M.A.; Arthur, R.B.; Lueders, E.E.; Breeding, W.P.; Patterson, H.H. The role of Copper (II) ions in Cu-BiOCl for use in the photocatalytic degradation of atrazine. *J. Environ. Chem. Eng.* **2018**, *6*, 5595–5601. [[CrossRef](#)]
108. Li, R.; Li, C. Chapter One—Photocatalytic Water Splitting on Semiconductor-Based Photocatalysts. In *Advances in Catalysis*; Song, C., Ed.; Academic Press: Cambridge, MA, USA, 2017; Volume 60, pp. 1–57.
109. Carboneras Contreras, M.B.; Villaseñor Camacho, J.; Fernández-Morales, F.J.; Cañizares, P.C.; Rodrigo Rodrigo, M.A. Biodegradability improvement and toxicity reduction of soil washing effluents polluted with atrazine by means of electrochemical pre-treatment: Influence of the anode material. *J. Environ. Manag.* **2020**, *255*, 109895. [[CrossRef](#)] [[PubMed](#)]
110. Saylor, G.L.; Zhao, C.; Kupferle, M.J. Synergistic enhancement of oxidative degradation of atrazine using combined electrolysis and ozonation. *J. Water Process Eng.* **2018**, *21*, 154–162. [[CrossRef](#)]
111. Zhou, S.; Bu, L.; Shi, Z.; Bi, C.; Yi, Q. A novel advanced oxidation process using iron electrodes and ozone in atrazine degradation: Performance and mechanism. *Chem. Eng. J.* **2016**, *306*, 719–725. [[CrossRef](#)]
112. Vera, Y.M.; Carvalho, R.J.d.; Torem, M.L.; Calfa, B.A. Atrazine degradation by in situ electrochemically generated ozone. *Chem. Eng. J.* **2009**, *155*, 691–697. [[CrossRef](#)]
113. Acero, J.L.; Stemmler, K.; von Gunten, U. Degradation Kinetics of Atrazine and Its Degradation Products with Ozone and •OH Radicals: A Predictive Tool for Drinking Water Treatment. *Environ. Sci. Technol.* **2000**, *34*, 591–597. [[CrossRef](#)]
114. Bianchi, C.L.; Pirola, C.; Ragaini, V.; Selli, E. Mechanism and efficiency of atrazine degradation under combined oxidation processes. *Appl. Catal. B Environ.* **2006**, *64*, 131–138. [[CrossRef](#)]
115. Yang, Y.; Cao, H.; Peng, P.; Bo, H. Degradation and transformation of atrazine under catalyzed ozonation process with TiO<sub>2</sub> as catalyst. *J. Hazard. Mater.* **2014**, *279*, 444–451. [[CrossRef](#)]
116. Yuan, X.; Xie, R.; Zhang, Q.; Sun, L.; Long, X.; Xia, D. Oxygen functionalized graphitic carbon nitride as an efficient metal-free ozonation catalyst for atrazine removal: Performance and mechanism. *Sep. Purif. Technol.* **2019**, *211*, 823–831. [[CrossRef](#)]
117. Ye, G.; Luo, P.; Zhao, Y.; Qiu, G.; Hu, Y.; Preis, S.; Wei, C. Three-dimensional Co/Ni bimetallic organic frameworks for high-efficient catalytic ozonation of atrazine: Mechanism, effect parameters, and degradation pathways analysis. *Chemosphere* **2020**, *253*, 126767. [[CrossRef](#)] [[PubMed](#)]
118. Gouma, S.; Fragoeiro, S.; Bastos, A.C.; Magan, N. 13—Bacterial and Fungal Bioremediation Strategies. In *Microbial Biodegradation and Bioremediation*; Das, S., Ed.; Elsevier: Oxford, UK, 2014; pp. 301–323.
119. Lasserre, J.-P.; Fack, F.; Revets, D.; Planchon, S.; Renaut, J.; Hoffmann, L.; Gutleb, A.C.; Muller, C.P.; Bohn, T. Effects of the Endocrine Disruptors Atrazine and PCB 153 on the Protein Expression of MCF-7 Human Cells. *J. Proteome Res.* **2009**, *8*, 5485–5496. [[CrossRef](#)] [[PubMed](#)]
120. Yanze-Kontchou, C.; Gschwind, N. Mineralization of the herbicide atrazine as a carbon source by a *Pseudomonas* strain. *Appl. Environ. Microbiol.* **1994**, *60*, 4297–4302. [[CrossRef](#)] [[PubMed](#)]
121. Struthers, J.K.; Jayachandran, K.; Moorman, T.B. Biodegradation of Atrazine by *Agrobacterium radiobacter* J14a and Use of This Strain in Bioremediation of Contaminated Soil. *Appl. Environ. Microbiol.* **1998**, *64*, 3368–3375. [[CrossRef](#)] [[PubMed](#)]
122. Bhatt, P.; Pathak, V.M.; Joshi, S.; Bisht, T.S.; Singh, K.; Chandra, D. Chapter 12—Major metabolites after degradation of xenobiotics and enzymes involved in these pathways. In *Smart Bioremediation Technologies*; Bhatt, P., Ed.; Academic Press: Cambridge, MA, USA, 2019; pp. 205–215.
123. Vidali, M. Bioremediation. An overview. *Pure Appl. Chem.* **2001**, *73*, 1163–1172. [[CrossRef](#)]
124. Hu, N.; Xu, Y.; Sun, C.; Zhu, L.; Sun, S.; Zhao, Y.; Hu, C. Removal of atrazine in catalytic degradation solutions by microalgae *Chlorella sp.* and evaluation of toxicity of degradation products via algal growth and photosynthetic activity. *Ecotoxicol. Environ. Saf.* **2021**, *207*, 111546. [[CrossRef](#)]
125. Qu, M.; Li, N.; Li, H.; Yang, T.; Liu, W.; Yan, Y.; Feng, X.; Zhu, D. Phytoextraction and biodegradation of atrazine by *Myriophyllum spicatum* and evaluation of bacterial communities involved in atrazine degradation in lake sediment. *Chemosphere* **2018**, *209*, 439–448. [[CrossRef](#)]
126. Newman, L.A.; Reynolds, C.M. Phytodegradation of organic compounds. *Curr. Opin. Biotechnol.* **2004**, *15*, 225–230. [[CrossRef](#)]
127. Murphy, I.J.; Coats, J.R. The capacity of switchgrass (*Panicum virgatum*) to degrade atrazine in a phytoremediation setting. *Environ. Toxicol. Chem.* **2011**, *30*, 715–722. [[CrossRef](#)]
128. Pérez, D.J.; Doucette, W.J.; Moore, M.T. Atrazine uptake, translocation, bioaccumulation and biodegradation in cattail (*Typha latifolia*) as a function of exposure time. *Chemosphere* **2022**, *287*, 132104. [[CrossRef](#)]
129. Zhu, X.Y. Study on Wastewater Treatment and Process Intensification by Pulsed High-Voltage Discharge. Ph.D. Thesis, Beijing University of Chemical Technology, Beijing, China, 2017.
130. Marotta, E.; Ceriani, E.; Schiorlin, M.; Ceretta, C.; Paradisi, C. Comparison of the rates of phenol advanced oxidation in deionized and tap water within a dielectric barrier discharge reactor. *Water Res.* **2012**, *46*, 6239–6246. [[CrossRef](#)]
131. Wang, Q.; Zhang, A.; Li, P.; Héroux, P.; Zhang, H.; Yu, X.; Liu, Y. Degradation of aqueous atrazine using persulfate activated by electrochemical plasma coupling with microbubbles: Removal mechanisms and potential applications. *J. Hazard. Mater.* **2021**, *403*, 124087. [[CrossRef](#)] [[PubMed](#)]
132. Aggelopoulos, C.A.; Tataraki, D.; Rassias, G. Degradation of atrazine in soil by dielectric barrier discharge plasma—Potential singlet oxygen mediation. *Chem. Eng. J.* **2018**, *347*, 682–694. [[CrossRef](#)]
133. Wang, J.; Wang, Z.; Vieira, C.L.Z.; Wolfson, J.M.; Pingtian, G.; Huang, S. Review on the treatment of organic pollutants in water by ultrasonic technology. *Ultrason. Sonochem.* **2019**, *55*, 273–278. [[CrossRef](#)]

134. Koskinen, W.C.; Sellung, K.E.; Baker, J.M.; Barber, B.L.; Dowdy, R.H. Ultrasonic decomposition of atrazine and alachlor in water. *J. Environ. Sci. Health Part B* **1994**, *29*, 581–590. [[CrossRef](#)]
135. Hiskia, A.; Ecke, M.; Troupis, A.; Kokorakis, A.; Hennig, H.; Papaconstantinou, E. Sonolytic, Photolytic, and Photocatalytic Decomposition of Atrazine in the Presence of Polyoxometalates. *Environ. Sci. Technol.* **2001**, *35*, 2358–2364. [[CrossRef](#)]
136. Kidak, R.; Dogan, S. Degradation of atrazine by advanced oxidation processes. In Proceedings of the Sixteenth International Water Technology Conference, Istanbul, Turkey, 7–10 May 2012.
137. Sivarajasekar, N.; Balasubramani, K.; Mohanraj, N.; Prakash Maran, J.; Sivamani, S.; Ajmal Koya, P.; Karthik, V. Fixed-bed adsorption of atrazine onto microwave irradiated Aegle marmelos Correa fruit shell: Statistical optimization, process design and breakthrough modeling. *J. Mol. Liq.* **2017**, *241*, 823–830. [[CrossRef](#)]
138. Hu, E.; Hu, Y.; Cheng, H. Performance of a novel microwave-based treatment technology for atrazine removal and destruction: Sorbent reusability and chemical stability, and effect of water matrices. *J. Hazard. Mater.* **2015**, *299*, 444–452. [[CrossRef](#)]
139. Chen, H.; Bramanti, E.; Longo, I.; Onor, M.; Ferrari, C. Oxidative decomposition of atrazine in water in the presence of hydrogen peroxide using an innovative microwave photochemical reactor. *J. Hazard. Mater.* **2011**, *186*, 1808–1815. [[CrossRef](#)] [[PubMed](#)]
140. Beltrán, F.J.; Ovejero, G.; Acedo, B. Oxidation of atrazine in water by ultraviolet radiation combined with hydrogen peroxide. *Water Res.* **1993**, *27*, 1013–1021. [[CrossRef](#)]
141. Hu, E.; Cheng, H. Catalytic effect of transition metals on microwave-induced degradation of atrazine in mineral micropores. *Water Res.* **2014**, *57*, 8–19. [[CrossRef](#)] [[PubMed](#)]
142. Wei, X.; Wu, Z.; Du, C.; Wu, Z.; Ye, B.-C.; Cravotto, G. Enhanced adsorption of atrazine on a coal-based activated carbon modified with sodium dodecyl benzene sulfonate under microwave heating. *J. Taiwan Inst. Chem. Eng.* **2017**, *77*, 257–262. [[CrossRef](#)]
143. Erdmann, F.; Ghantous, A.; Schüz, J. Environmental Agents and Childhood Cancer. In *Encyclopedia of Environmental Health*, 2nd ed.; Nriagu, J., Ed.; Elsevier: Oxford, UK, 2019; pp. 347–359.
144. Khan, J.A.; Shah, N.S.; Khan, H.M. Decomposition of atrazine by ionizing radiation: Kinetics, degradation pathways and influence of radical scavengers. *Sep. Purif. Technol.* **2015**, *156*, 140–147. [[CrossRef](#)]
145. Xu, G.; Yao, J.-z.; Tang, L.; Yang, X.-y.; Zheng, M.; Wang, H.; Wu, M.-h. Electron beam induced degradation of atrazine in aqueous solution. *Chem. Eng. J.* **2015**, *275*, 374–380. [[CrossRef](#)]
146. Govantes, F.; Porrúa, O.; García-González, V.; Santero, E. Atrazine biodegradation in the lab and in the field: Enzymatic activities and gene regulation. *Microb. Biotechnol.* **2009**, *2*, 178–185. [[CrossRef](#)] [[PubMed](#)]
147. Shapir, N.; Mongodin, E.F.; Sadowsky, M.J.; Daugherty, S.C.; Nelson, K.E.; Wackett, L.P. Evolution of Catabolic Pathways: Genomic Insights into Microbial *s*-Triazine Metabolism. *J. Bacteriol.* **2007**, *189*, 674–682. [[CrossRef](#)] [[PubMed](#)]
148. de Souza, M.L.; Sadowsky, M.J.; Wackett, L.P. Atrazine chlorohydrolase from *Pseudomonas* sp. strain ADP: Gene sequence, enzyme purification, and protein characterization. *J. Bacteriol.* **1996**, *178*, 4894–4900. [[CrossRef](#)]
149. Shapir, N.; Pedersen, C.; Gil, O.; Strong, L.; Seffernick, J.; Sadowsky Michael, J.; Wackett Lawrence, P. TrzN from *Arthrobacter aurescens* TC1 Is a Zinc Amidohydrolase. *J. Bacteriol.* **2006**, *188*, 5859–5864. [[CrossRef](#)] [[PubMed](#)]
150. Seffernick Jennifer, L.; Johnson, G.; Sadowsky Michael, J.; Wackett Lawrence, P. Substrate Specificity of Atrazine Chlorohydrolase and Atrazine-Catabolizing Bacteria. *Appl. Environ. Microbiol.* **2000**, *66*, 4247–4252. [[CrossRef](#)] [[PubMed](#)]
151. Seffernick Jennifer, L.; Aleem, A.; Osborne Jeffrey, P.; Johnson, G.; Sadowsky Michael, J.; Wackett Lawrence, P. Hydroxyatrazine *N*-Ethylaminohydrolase (*AtzB*): An Amidohydrolase Superfamily Enzyme Catalyzing Deamination and Dechlorination. *J. Bacteriol.* **2007**, *189*, 6989–6997. [[CrossRef](#)] [[PubMed](#)]
152. Shapir, N.; Osborne Jeffrey, P.; Johnson, G.; Sadowsky Michael, J.; Wackett Lawrence, P. Purification, Substrate Range, and Metal Center of *AtzC*: The *N*-Isopropylammelide Aminohydrolase Involved in Bacterial Atrazine Metabolism. *J. Bacteriol.* **2002**, *184*, 5376–5384. [[CrossRef](#)] [[PubMed](#)]
153. Rousseaux, S.; Hartmann, A.; Soulas, G. Isolation and characterisation of new Gram-negative and Gram-positive atrazine degrading bacteria from different French soils. *FEMS Microbiol. Ecol.* **2001**, *36*, 211–222. [[CrossRef](#)] [[PubMed](#)]
154. García-González, V.; Govantes, F.; Porrúa, O.; Santero, E. Regulation of the *Pseudomonas* sp. Strain ADP Cyanuric Acid Degradation Operon. *J. Bacteriol.* **2005**, *187*, 155–167. [[CrossRef](#)]
155. Karns Jeffrey, S. Gene Sequence and Properties of *ans*-Triazine Ring-Cleavage Enzyme from *Pseudomonas* sp. Strain NRRLB-12227. *Appl. Environ. Microbiol.* **1999**, *65*, 3512–3517. [[CrossRef](#)] [[PubMed](#)]
156. Getenga, Z.; Dörfler, U.; Iwobi, A.; Schmid, M.; Schroll, R. Atrazine and terbuthylazine mineralization by an *Arthrobacter* sp. isolated from a sugarcane-cultivated soil in Kenya. *Chemosphere* **2009**, *77*, 534–539. [[CrossRef](#)] [[PubMed](#)]
157. Bahena, C.L.; Martínez, S.S.; Guzmán, D.M.; del Refugio Trejo Hernández, M. Sonophotocatalytic degradation of alazine and gesaprim commercial herbicides in TiO<sub>2</sub> slurry. *Chemosphere* **2008**, *71*, 982–989. [[CrossRef](#)] [[PubMed](#)]
158. Wen, D.; Chen, B.; Liu, B. An ultrasound/O<sub>3</sub> and UV/O<sub>3</sub> process for atrazine manufacturing wastewater treatment: A multiple scale experimental study. *Water Sci. Technol.* **2021**, *85*, 229–243. [[CrossRef](#)]
159. Sarmiento, S.M.; Miranda, J.T.G. Kinetics of the atrazine degradation process using H<sub>2</sub>O<sub>2</sub>-UVC. *Water Sci. Technol.* **2014**, *69*, 2279–2286. [[CrossRef](#)]
160. Popova, S.A.; Matafonova, G.G.; Batoev, V.B. Removal of organic micropollutants from water by sonophotolytic-activated persulfate process. *IOP Conf. Ser. Mater. Sci. Eng.* **2019**, *687*, 066051. [[CrossRef](#)]



161. Moreira, A.J.; Borges, A.C.; Gouvea, L.F.C.; MacLeod, T.C.O.; Freschi, G.P.G. The process of atrazine degradation, its mechanism, and the formation of metabolites using UV and UV/MW photolysis. *J. Photochem. Photobiol. A Chem.* **2017**, *347*, 160–167. [[CrossRef](#)]
162. Moreira, A.J.; Pinheiro, B.S.; Araújo, A.F.; Freschi, G.P.G. Evaluation of atrazine degradation applied to different energy systems. *Environ. Sci. Pollut. Res.* **2016**, *23*, 18502–18511. [[CrossRef](#)] [[PubMed](#)]
163. Tauber, A.; von Sonntag, C. Products and Kinetics of the OH-radical-induced Dealkylation of Atrazine. *Acta Hydrochim. Hydrobiol.* **2000**, *28*, 15–23. [[CrossRef](#)]
164. Song, W.; Li, J.; Fu, C.; Wang, Z.; Zhang, X.; Yang, J.; Hogland, W.; Gao, L. Kinetics and pathway of atrazine degradation by a novel method: Persulfate coupled with dithionite. *Chem. Eng. J.* **2019**, *373*, 803–813. [[CrossRef](#)]
165. Khan, J.A.; He, X.; Shah, N.S.; Sayed, M.; Khan, H.M.; Dionysiou, D.D. Degradation kinetics and mechanism of desethyl-atrazine and desisopropyl-atrazine in water with  $\bullet\text{OH}$  and  $\text{SO}_4^-$  based-AOPs. *Chem. Eng. J.* **2017**, *325*, 485–494. [[CrossRef](#)]
166. Yanagisawa, I.; Oyama, T.; Serpone, N.; Hidaka, H. Successful Scission of a Recalcitrant Triazinic Ring. The Photoassisted Total Breakup of Cyanuric Acid in Ozonized  $\text{TiO}_2$  Aqueous Dispersions in the Presence of an Electron Acceptor ( $\text{H}_2\text{O}_2$ ). *J. Phys. Chem. C* **2008**, *112*, 18125–18133. [[CrossRef](#)]
167. Ding, X.; Wang, S.; Shen, W.; Mu, Y.; Wang, L.; Chen, H.; Zhang, L. Fe@Fe<sub>2</sub>O<sub>3</sub> promoted electrochemical mineralization of atrazine via a triazinon ring opening mechanism. *Water Res.* **2017**, *112*, 9–18. [[CrossRef](#)]
168. Borràs, N.; Oliver, R.; Arias, C.; Brillas, E. Degradation of Atrazine by Electrochemical Advanced Oxidation Processes Using a Boron-Doped Diamond Anode. *J. Phys. Chem. A* **2010**, *114*, 6613–6621. [[CrossRef](#)]
169. World Health Organization. *Pesticide Residues in Food: 2007, Toxicological Evaluations, Sponsored Jointly by FAO and WHO, with the support of the International Programme on Chemical Safety, Joint Meeting of the FAO Panel of Experts on Pesticide Residues in Food and the Environment and the WHO Core Assessment Group*; World Health Organization: Geneva, Switzerland, 2007.
170. Ralston-Hooper, K.; Hardy, J.; Hahn, L.; Ochoa-Acuña, H.; Lee, L.S.; Mollenhauer, R.; Sepúlveda, M.S. Acute and chronic toxicity of atrazine and its metabolites deethylatrazine and deisopropylatrazine on aquatic organisms. *Ecotoxicology* **2009**, *18*, 899–905. [[CrossRef](#)]
171. Stratton, G.W. Effects of the herbicide atrazine and its degradation products, alone and in combination, on phototrophic microorganisms. *Arch. Environ. Contam. Toxicol.* **1984**, *13*, 35–42. [[CrossRef](#)]
172. EFSA Panel on Contaminants in the Food Chain (CONTAM); EFSA Panel on Food Contact Materials; Enzymes, Flavourings and Processing Aids (CEF). Scientific Opinion on Melamine in Food and Feed. *EFSA J.* **2010**, *8*, 1573. [[CrossRef](#)]
173. Sánchez, V.; López-Bellido, F.J.; Cañizares, P.; Rodríguez, L. Assessing the phytoremediation potential of crop and grass plants for atrazine-spiked soils. *Chemosphere* **2017**, *185*, 119–126. [[CrossRef](#)] [[PubMed](#)]
174. Arnold, S.M.; Hickey, W.J.; Harris, R.F. Degradation of Atrazine by Fenton's Reagent: Condition Optimization and Product Quantification. *Environ. Sci. Technol.* **1995**, *29*, 2083–2089. [[CrossRef](#)] [[PubMed](#)]